

Impact of potential and actual evapotranspiration on drought phenomena over water and energy-limited regions

by

Shaik Rehana, Monish N.T.

in

Theoretical and Applied Climatology

Report No: IIIT/TR/2021/-1



Centre for Spatial Informatics
International Institute of Information Technology
Hyderabad - 500 032, INDIA
January 2021



Impact of potential and actual evapotranspiration on drought phenomena over water and energy-limited regions

S. Rehana¹ · N. T. Monish¹

Received: 12 June 2020 / Accepted: 4 January 2021

© The Author(s), under exclusive licence to Springer-Verlag GmbH, AT part of Springer Nature 2021

Abstract

Understanding the relevance of potential (PET) and actual evapotranspiration (AET) in the drought characterization over energy and water-limited regions is unexplored. The present study tries to restructure the Standardized Precipitation Evapotranspiration Index (SPEI) with AET to represent the anomalies of actual water availability in addition to precipitation over India. The AET is estimated using the Budyko hypothesis at annual scale which was validated with Global Land Evaporation Amsterdam Model (GLEAM) satellite-based AET data. AET-based drought index was in more agreement with remote sensing-based drought severity index (DSI) for major drought events compared to PET-based drought index for water-limited zone compared to energy-limited. For water-limited zones, the PET-based drought index has overestimated the drought intensities, while for energy-limited zones such effect is not significant. AET-based drought index has estimated lesser areal extents under extreme drought conditions compared to PET-based drought index for water-limited zones of India. The rate of increase of drought frequencies was noted to be higher with AET for extreme droughts when compared to other categories. Overall, considerable differences in drought characteristics based on PET and AET drought indices over water-limited zones of India stresses on the use of AET in the drought assessment instead of PET.

1 Introduction

Drought is a natural hazard which is expected due to the deviation of a hydro-meteorological variable (e.g., rainfall, runoff, and soil moisture) from the long-term average conditions affecting millions of people all around the world (Dai 2011; Sheffield et al. 2012). Various drought monitoring tools have been evolved to study various forms of droughts (meteorological, hydrological, and agricultural) by considering various hydro-meteorological variables (rainfall, runoff, and soil moisture). Meteorological drought plays a major role in the drought forecasting, assessment, and monitoring by several government agencies. In this context, characterization of drought in terms of severity, frequency, areal extent, and duration is of relevance which is conventionally performed using various meteorological drought indices such as Standardized

Precipitation Index (SPI) (McKee et al. 1993) and Standardized Precipitation Evapotranspiration Index (SPEI) (El Kenawy et al. 2010; Vicente Serrano et al. 2010; Vicente-Serrano et al. 2010) (Table 1). Several studies adopted various indices to evaluate drought events for Indian subcontinent for current and under climate change signals (Aadhar and Mishra 2017; Kumar et al. 2013; Mallya et al. 2016; Nath et al. 2017) as given in Table 1. The SPEI has gained much attention in the research community due to its capability to account for atmospheric water demand in terms of difference between precipitation (P) and potential evapotranspiration (PET), (P-PET) in the drought characterization as proposed by (Vicente Serrano et al. 2010). The PET-based drought formulation of SPEI has been identified as a reliable measure in the drought characterization compared to solely on precipitation (Spinoni et al. 2019). The PET-based drought indices, however, cannot account for the actual atmospheric water demand and variations of land and vegetation (Liu et al. 2016), whereas the actual evapotranspiration (AET) represents the transfer of moisture from the land surface to the atmosphere in response to both energy demand and moisture supply (Shelton 2008). Therefore, inclusion of AET in the drought estimation can account for the actual water

✉ S. Rehana
rehana.s@iiit.ac.in

¹ Spatial Informatics, International Institute of Information Technology, Gachibowli, Hyderabad 500032, India

Table 1 Summary of past studies conducted on the Indian drought characteristics using various drought indices

Author and year	Spatial scale of analysis	Data and resolution	Drought indices and variables used	Major findings
Bhalme and Mooley (1980)	33 meteorological subdivisions of India	Monthly sub divisional rainfall data from 1891 to 1975	Drought Area Index based on rainfall	Large number of monsoon breaks and shifts in the monsoon and weak meridional pressure gradients are the major factors for the occurrence of large-scale droughts
Parthasarathy et al. (1987)	29 meteorological subdivisions of India	Monthly homogeneous rainfall data from 1971 to 1984	Percentage of rainfall departure from normal as per IMD	The probabilities of occurrence of droughts/floods are high in Haryana, Punjab, west Rajasthan, Gujarat and Saurashtra, and Kutch subdivisions
Singh (2001)	All over India	Daily monsoon season precipitation data from 1940 to 1980	Percentage of rainfall departure from normal as per IMD	During drought years the monsoon rainfall amount decreases all over India but significant reduction over central and west coast
Guhathakurta (2003)	424 districts covering all over India	Daily rainfall data from 1988 to 2001	Percentage of rainfall departure from normal as per IMD	37.5% of the districts were affected by drought per year
Chaudhari and Dadhwal (2004)	36 meteorological subdivisions of India	Monthly rainfall data from 1971 to 2002	SPI based on Rainfall	26 subdivisions were having rainfall below normal and six were very severely affected; SPI served as a good index for regional crop production in India
Kumar et al. (2013)	All over India	$1^\circ \times 1^\circ$ daily gridded data from 1901 to 2010 from IMD	SPEI based on rainfall and PET	The major portion of the drought variability over India is influenced by El Nino/Southern Oscillation (ENSO); warming of equatorial Indian Ocean is responsible for the observed increase in intensity of droughts during the recent decades
Shah and Mishra (2014)	All over India	IMD daily gridded data at $0.25^\circ \times 0.25^\circ$ from 1901 to 2010; IMD daily maximum and minimum temperature data at $1^\circ \times 1^\circ$ from 1969 to 2005	SPI, SRI, SSI based on rainfall, runoff and soil moisture	Development of near real-time drought monitor for India
Das et al. (2015)	4 homogeneous meteorological zones	Monthly gridded SPEI data at $0.5^\circ \times 0.5^\circ$ from 1901 to 2008 extracted from global SPEI data base based on version 3.2 of the Climatic Research Unit (CRU) dataset	SPEI based on Rainfall and PET	Significant increasing trends of drought duration and magnitude during the monsoon was found over parts of eastern, central, and northeastern regions; decreasing trends over west coast, arid western regions, and north India

Table 1 (continued)

Author and year	Spatial scale of analysis	Data and resolution	Drought indices and variables used	Major findings
Mishra et al. (2017)	All over India	India, IMD ($0.25^\circ \times 0.25^\circ$) gridded data (1951–2015)	SPI, SSI based on rainfall and soil moisture	Differences in drought characteristics simulated by the three models (VIC, NOAA, and CLM), multimodel ensemble mean can be a better estimate of agricultural droughts over India
Ganeshchandra et al. (2016)	All over India	India, IMD ($1^\circ \times 1^\circ$) gridded data (1901–2004)	SPI, SPEI, HMM-DI ^a , GMM-DI ^b based on rainfall and PET	An increased duration, severity, and spatial extent of droughts in the recent decades and identify the Indo-Gangetic plain, parts of coastal south India, and central Maharashtra as vulnerable regions for recent droughts
Nath et al., (2017)	Indo-Gangetic Plain of India	Climatic Research Unit of University of East Anglia ($0.5^\circ \times 0.5^\circ$) (1961–2012) and CMIP5 datasets for 27 coupled climate models (2006–2099)	SPEI based on Rainfall and PET	Both precipitation and PET are projected to increase, and therefore drought and flood incidences will also predicted to increase in the future

SRI Standardized Runoff Index, SSI Standardized Streamflow Index, VIC Variable Infiltration Capacity, NOAA National Oceanic and Atmospheric Administration, CLM Community Land Model

^a NOAA

^b CLM

availability or residual amount of water available in addition to precipitation. Few authors attempted to use AET explicitly in the formulation of drought characterization (Kim & Rhee, 2016). The efforts made in the literature to include AET in the drought indices are Drought Severity Index (DSI) (Mu et al., 2012) and U.S. Drought Monitor (USDM) (Svoboda et al., 2002). Kim and Rhee (2016) developed the Standardized Evapotranspiration Deficit Index (SEDI) using the AET estimated from the Bouchet hypothesis and the structure of SPEI as a fully ET-based drought index without consideration of precipitation. The use of AET in the formulation of SPEI has been tried by few researchers (Dai, 2011; Homdee et al., 2016; Joetzjer et al., 2013; Liu et al., 2016). Homdee et al. (2016) compared SPEI with AET-based drought indices, where AET was modeled based on SWAT (Soil and Water Assessment Tool). However, hydrological model-driven AET-induced drought indices will provide a limitation over the applicability over large spatial scales given with the rigorous catchment characteristic requirement. Liu et al. (2017) adopted dynamic parameter Budyko hypothesis to estimate AET in the development of drought index, Standardized Wetness Index (SWI), as the ratio of residual available water (P-AET) and energy (PET-AET) with SPEI as basic mathematical formulation. However, application of such dynamic Budyko model requires accurate measurements of runoff data at finer resolution. Furthermore, the suitability of use of PET and AET in the formulation of SPEI has been tested for both humid and arid climates by (Begueria et al., 2014). Additionally, most of the earlier drought assessment studies with SPEI for Indian subcontinent were based on PET (e.g., Kumar et al., 2013; Mallya et al., 2016; Nath et al., 2017). Suitability of AET, which can account for both water and energy based evaporative demands, in drought characterization is unexplored for Indian context. The present study made an effort to use AET in the formulation of SPEI to study various drought characteristics all over India. The AET is estimated using the Budyko hypothesis, a robust classical model for the estimation of AET relating long-term-average water and energy balances at catchment scales relating precipitation and PET (Budyko, 1974). It can be noted that as the Budyko approach of estimation of AET workability is suitable for long-term-average scale, the study mainly focused on 12-month time scale (annual drought) characterization. In order to guarantee the relevance of AET-based drought index for Indian context and to avoid the use of short-term soil moisture storages, the focus will be only on 12-month drought characterization in terms of areal extent, frequency, intensity, and duration. The study used fine-resolution rainfall and temperature data provided by India Meteorological Department (IMD). The annual scale drought-induced modeled using AET is named as Standardised Precipitation Actual Evapotranspiration Index (SPA EI). The newly framed drought index has been validated with most advanced state-of-the-art satellite-based datasets. The annual scale AET estimated using the Budyko approach has

been tested with Global Land Evaporation Amsterdam Model (GLEAM) satellite-based AET data. Further, the AET-based drought index of SPA EI was tested with remote sensing-based DSI to evaluate the performance over water and energy-limited regions of India. Moreover, the study analyzed various drought characteristics of frequency, areal extent, severity, and drought duration along with evaluation of such drought characteristics for three time periods of 1951–1971, 1972–1992, and 1993–2013 with fine resolution of $0.25 \times 0.25^\circ$ observed meteorological data for India.

2 Materials and methods

2.1 Estimation of AET

The drought index, SPEI, is based on the climatic water balance, the accumulated monthly difference (in mm) between precipitation and PET as follows:

$$RAW_{PET} = P - PET \quad (1)$$

where P is the monthly precipitation (mm) and PET is the monthly potential evapotranspiration (mm). The estimated D values represents the water demand or surplus (P-PET), while the evapotranspiration is the result of complex relationship between atmosphere and surface water available, vegetation, and soil characteristics (Brutsaert, 1982). Conventionally, it is assumed that available water and energy are the primary factors affecting the rate of evapotranspiration (Budyko, 1974). In this context, the use of PET in the drought assessment studies may not be able to include the actual surface available moisture. Further, the AET includes the interception, actual soil evaporation and actual plant transpiration (Homdee et al., 2016). If the difference between precipitation and AET is considered, it can account for the actual residual available water (RAW) or water budget during drought conditions.

$$RAW_{AET} = P - AET \quad (2)$$

The original formulation of SPEI used the Thornthwaite model, which calculates PET based on the mean temperatures. Most of the earlier SPEI-based drought studies all over India were also based on the Thornthwaite model (Kumar et al., 2013; Mallya et al., 2016). The Thornthwaite model tends to underestimate PET in arid and semi-arid regions (Jensen et al., 1990) and overestimate PET in humid and tropical regions (Schrier et al., 2011). The Hargreaves equation (Hargreaves, 1975; Hargreaves & Allen, 2003) strikes a balance between minimum data requirements and accurate PET estimation (Stagge et al., 2014). The present study employed the Hargreaves equation for PET calculation which requires minimum, maximum, and mean temperatures along with the geographical location of the region as follows:

$$\text{PET} = 0.0023 \times (T_{\max} - T_{\min})^{\frac{1}{2}} \times (T_{\text{mean}} + 17.8) \times R_a \quad (3)$$

where T_{\max} , T_{\min} , and T_{mean} represent the maximum, minimum, and mean temperatures respectively, whereas R_a is the extra-terrestrial radiation expressed in equivalent evaporation units and calculated using the latitude of the location and time of the year.

To calculate SPAEI, accurate estimates of AET will be essential, which is more complex compared to PET estimation. The conventional ways of estimation of AET includes, water budget (difference (P-R) between precipitation (P) and runoff (R)) at annual and catchment scales (Twine et al. 2004). Furthermore, satellite-based AET data also has been evolved for developing spatially and temporally fine terrestrial AET data by integrating surface energy models (Kalma et al., 2008). However, direct measurements of AET for Indian case study are scarce and global datasets (Mueller et al., 2011) have limitations over the spatio-temporal data availability and validation, while interest towards more simple and robust approaches to estimate AET have also gained much attention which can use readily available operational meteorological variables of precipitation, temperature, PET, etc. (Zhang et al., 2004). Furthermore, the study emphasizes the use of common operational high-resolution meteorological data obtained by IMD in AET estimation all over India. In this context, one of the conventional methods to estimate AET in hydrology for many years is to estimate PET first and then applying a limiting factor to account for the water availability and soil (Anabalón & Sharma, 2017). To this end, several empirical models have been developed for estimating AET which are based on the assumption that AET is limited by the water availability in terms of precipitation under very dry conditions and energy availability in terms of PET under very wet conditions (Budyko, 1974; Zhang et al., 2004). Budyko (1974) has developed a relationship between three hydro-climatic variables for a basin: P , PET, and AET. Budyko hypothesis states that the ratio of the AET over precipitation (AET/ P) is fundamentally related to the ratio of the PET over precipitation (PET/ P) as follows:

$$\frac{\text{AET}}{P} = 1 + \frac{\text{PET}}{P} - \left(1 + \left(\frac{\text{PET}}{P} \right)^{\omega} \right)^{(1/\omega)} \quad (4)$$

Fu's parameter ω accounts for the effects of climate variability, basin characteristics such as soil, vegetation, and terrain (Donohue et al., 2007). The Budyko framework provides a simple and powerful tool to estimate the AET on multiyear time scales (Bai et al., 2020). There are several advancements has been made over the Budyko formulation including single parameter by Fu (1981) or more parameters by Choudhury (1999). As the study was aimed for the implementation at climate regional scale and due to the lack of streamflow data at a finer resolution, the study has considered a non-parametric

formulation, which allows a direct implementation with minimum data. One such non-parametric formulation which has been widely used is by Zhang et al. (2004) for estimating AET, which is given as follows:

$$\text{AET} = \left[P \left(1 - \exp \left(\frac{-\text{PET}}{P} \right) \right) \text{PET} \tanh \left(\frac{P}{\text{PET}} \right) \right]^{0.5} \quad (5)$$

It can be noted that any such other non-parametric formulations can be implemented in the analysis which can account for the soil moisture and storage anomalies in the estimation of AET.

The original Budyko equation (Eq. 5) has been developed for a long-time scale (Budyko, 1974; Zhou et al., 2015). However, the Budyko framework can be applied over short periods of monthly and annual scales (Buytaert & Bièvre, 2012; M. Liu et al., 2017), if the parameter ω , which represents the joint effect of climate and land surface is estimated. For a reasonable application of the Budyko equation as developed by Zhang et al. (2004) (Eq. 5), we used a 12-month scale for the estimation of drought indices. Estimation of ω based on the observed AET and P values is beyond the scope of the present study. The main emphasis of the study is to compare the applicability of AET in the drought characterization for Indian subcontinent.

Therefore, Budyko equation is subjected to the following boundary conditions (Sposito, 2017) as follows:

$$\text{AET} \rightarrow \text{PET} \text{ as } P \uparrow \infty (\text{energy supply is limiting}) \quad (6)$$

$$\text{AET} \rightarrow P \text{ as } \text{PET} \uparrow \infty (\text{water supply is limiting}) \quad (7)$$

That is for energy-limited regions, the AET is defined by PET and for water-limited regions the AET is defined by P . Given this, there will not be any difference between the PET and AET-based drought indices for energy-limited regions, whereas such differences for water-limited zones are more evident compared to energy-limited regions.

As the workability of AET model applied in the present study, which is based on the Budyko formulation, is more towards annual scales, the study worked to estimate the 12-month scale drought indices. The monthly rainfall and PET are accumulated to 12-month scale as follows:

$$P_i^k = \sum_{i-k+1}^i P_i \text{ where } k = 12 \quad (8)$$

$$\text{PET}_i^k = \sum_{i-k+1}^i \text{PET}_i \text{ where } k = 12 \quad (9)$$

where P_i^k and PET_i^k are the accumulated rainfall and PET in month, i . The 12-month accumulated P and PET values will be used in Eq. 5 to estimate the accumulated AET values at 12-month scale. By applying accumulated values of P and PET directly in the Eq. 5, the conditions of P as zero for any given month can overcome in the calculation.

After the calculation of accumulated PET and AET, the accumulated RAW values were calculated for estimating SPAEI, as follows:

$$\text{RAW}_i^{12} = P_i^{12} - \text{AET}_i^{12} \quad (10)$$

2.2 Fitting different probability distributions for (P-PET) and (P-AET)

The SPEI formulation necessitates fitting of an appropriate parametric probability distribution for the transformation of accumulated estimates of (P-PET) into standard normal distribution. The choice of an inappropriate probability distribution may lead to bias in the index values leading to inaccurate drought indices (Sienz et al., 2012; Stagge et al., 2015). Moreover, most of the earlier drought studies all over India were based on the original structure of SPEI formulation by Vicente Serrano et al. (2010) following three-parameter log-logistic (LL) distribution. However, Stagge et al. (2015) recommended generalized extreme value (GEV) distribution for formulating the SPEI. Few more studies (e.g., Homdee et al., 2016) also revealed that GEV distribution fits well for the climatic water balance. Also, Wang et al. (2019) noted that Pearson type III (PT-III) distribution is a reliable distribution for formulating SPEI over China. The performance of candidate distributions to fit SPEI/SPAEI was tested with GEV, LL, PT-III, and normal distributions over Indian land mass for various meteorologically homogeneous regions was studied by Monish and Rehana (2019). Based on the Akaike information criterion (AIC) (Akaike, 1974), the GEV distribution was identified as the best fit with more than 50.26% of grid points for 12-month time scale of SPEI values for all over India in the study by Monish and Rehana (2019). The present study compared GEV and LL distributions for formulating the SPAEI for 12-month time scale.

2.2.1 Generalized extreme value distribution

GEV distribution comes under the family of extreme value theory, which is the limiting distribution for an observed variable of maximum or minimum values that are independent and identically distributed. The probability density function ($f(x)$) of the three-parameter GEV distribution is given as follows:

$$f(x) = \begin{cases} \left(\frac{1}{\sigma}\right) \left[1 + \xi z(x)\right]^{-1/\xi} e^{-\left[1 + \xi z(x)\right]^{-1/\xi}}, & \xi \neq 0, 1 + \xi z(x) > 0 \\ \left(\frac{1}{\sigma}\right) e^{-z(x) - e^{-z(x)}}, & \xi = 0, -\infty < x < \infty \end{cases} \quad (11)$$

where

$$z(x) = \frac{x - \mu}{\sigma} \quad (12)$$

where μ , σ , and ξ are the location, scale, and shape parameters respectively which are estimated using the maximum likelihood method. The cumulative distribution function (CDF), $F(x)$, for GEV can be calculated as follows:

$$F(x) = e^{-t(x)} \quad (13)$$

where

$$t(x) = \begin{cases} \left(1 + \xi \left(\frac{x - \mu}{\sigma}\right)\right)^{-\frac{1}{\xi}} & \text{if } \xi \neq 0 \\ e^{-x/\sigma} & \text{if } \xi = 0 \end{cases} \quad (14)$$

2.2.2 Three-parameter log-logistic distribution

The probability density function ($f(x)$) of the three-parameter log-logistic distribution is given as follows:

$$f(x) = \frac{\beta}{\alpha} \left(\frac{X - \gamma}{\alpha}\right)^{\beta - 1} \left[1 + \left(\frac{X - \gamma}{\alpha}\right)^{\beta}\right]^{-2} \quad (15)$$

where α , β , and γ are the scale, shape, and origin parameters respectively which are obtained by the following L-moments procedure:

$$\beta = \frac{2w_1 - w_0}{6w_1 - w_0 - 6w_2} \quad (16)$$

$$\alpha = \frac{(w_0 - 2w_1)\beta}{\Gamma(1 + 1/\beta)\Gamma(1 - 1/\beta)} \quad (17)$$

$$\gamma = w_0 - \alpha\Gamma(1 + 1/\beta)\Gamma(1 - 1/\beta) \quad (18)$$

where w_0 , w_1 , and w_2 are the probability weighted moments calculated based on method by Sheng and Hashino (2007), as follows:

$$W_r = \frac{1}{n} \binom{n-1}{r}^{-1} \sum_{j=1}^{n-r} \binom{n-j}{r} x_j \quad r = 0, 1, 2 \quad (19)$$

where n is the sample size and x_j is the ordered vector of observations in descending order.

Next, the cumulative distribution function of log-logistic distribution can be calculated with the estimated parameters as:

$$F(x) = \left[1 + \left(\frac{X - \gamma}{\alpha}\right)^{\beta}\right]^{-1} \quad (20)$$

2.3 Performance evaluation criteria for SPEI and SPAEI

The best probability distribution for fitting the values of RAW_{PET} and RAW_{AET} in the formulation of SPEI and SPAEI value can be selected based on (i) Kolmogorov–Smirnov (K-S) goodness-of-fit tests to study the distance measured between selected distribution and the empirical distributions (ii) AIC likelihood ratio tests which is based on the information criteria for relative ranking of the distributions (e.g., AIC test). In the present study, two performance evaluation criteria, K-S goodness-of-fit and AIC statistical method (Akaike 1974), are used to select the most appropriate candidate distribution in the formulation of SPEI and SPAEI for meteorologically homogeneous zones and overall India at 12-month time scales.

2.3.1 Kolmogorov–Smirnov test

The K-S goodness-of-fit test estimates the maximum difference between the theoretical and empirical cumulative distribution of sampled points. If x_1, \dots, x_n are the random samples from a candidate distribution with CDF ($F(x)$), the empirical CDF can be estimated as

$$F_n(x) = \frac{\text{number of observations} \leq x}{n} \tag{21}$$

The K-S test statistic will be based on the largest vertical difference (Δ) between the theoretical and empirical CDFs of candidate distribution.

$$\Delta = \max |F_n(x) - F(x)| \tag{22}$$

The hypothesis that the data follows a particular distribution will be rejected if the test statistic, Δ , is greater than the critical value obtained from the standard table for a given significance level (Chakravarty et al. 1967).

2.3.2 Akaike information criterion

AIC works by capturing the bias of fit and unreliability from the number of model parameters. According to AIC criterion, each probability distribution will be ranked and best probability distribution function will be selected with minimum AIC value. The AIC values were estimated for both RAW_{PET} and RAW_{AET} for each grid point all over India.

$$AIC = 2k - 2\ln(L) \tag{23}$$

where k is the number of parameters of a probability distribution and L is the maximized value of the likelihood function for the distribution.

2.4 Estimation of SPAEI

The basic structure of SPEI has been followed to test the AET-based drought index of SPAEI. The original formulation of SPEI works by selecting the cumulative distribution function (CDF) values, $F(x)$, for the selected probability distribution function. The SPEI values were calculated as follows:

Fig. 1 Meteorological homogeneous zones of India

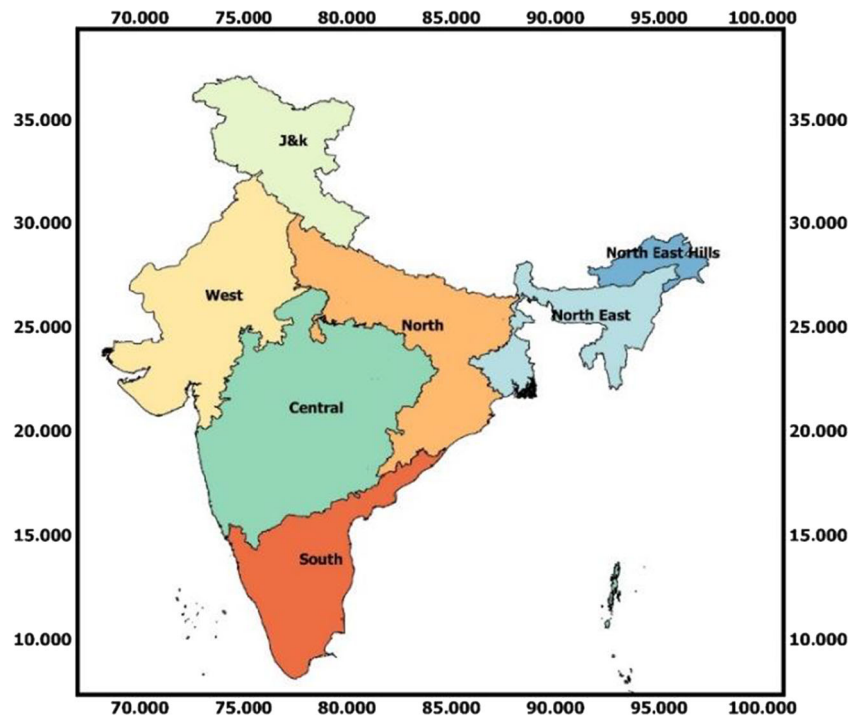


Table 2 K–S rejection frequencies (%) for the probability distributions of generalized extreme value (GEV) and 3-parameter log–logistic distributions for various homogeneous zones and all over India for SPEI and SPAEI (values in the bracket) at 12-month accumulation period

Distribution	North	South	Central	West	NE	NE hills	J&K	India
GEV	2.91 (9.85)	11.16 (6.13)	7.07 (8.67)	4.11 (49.63)	15.31 (8.33)	30.70 (18.11)	35.16 (37.91)	10.00 (19.48)
Log–logistic	3.52 (17.63)	4.08 (12.89)	6.62 (23.05)	9.06 (85.58)	9.23 (14.11)	29.92 (40.94)	35.71 (45.60)	9.09 (34.63)

$$SPEI = W - \frac{C_0 + C_1 W + C_2 W^2}{1 + d_1 W + d_2 W^2 + d_3 W^3} \tag{24}$$

$$\text{where } W = \sqrt{-2\ln(p)} \text{ for } P \leq 0.5 \tag{25}$$

where P is the probability of exceeding a determined RAW value, $P = 1 - F(x)$. If $P > 0.5$, then P is replaced by $(1 - P)$ and the sign of the resultant SPAEI is reversed. The constants

are $C_0 = 2.5515517$, $C_1 = 0.802583$, $C_2 = 0.010328$, $d_1 = 1.432788$, $d_2 = 0.189269$, and $d_3 = 0.001308$. By substituting the C_0 , C_1 , and C_2 values in Eq. 13, we calculate the SPEI/SPAEI values at 12-month scale. The drought severity was identified using the SPEI/SPAEI ranges as described by Vicente-Serrano et al. (2010) as follows: A drought event was classified as moderate if SPEI/SPAEI between -1.0 and -1.49 , severe if SPEI/SPAEI was between -1.50 and -1.99 , and extreme if SPEI/SPAEI was less than -2.0 .

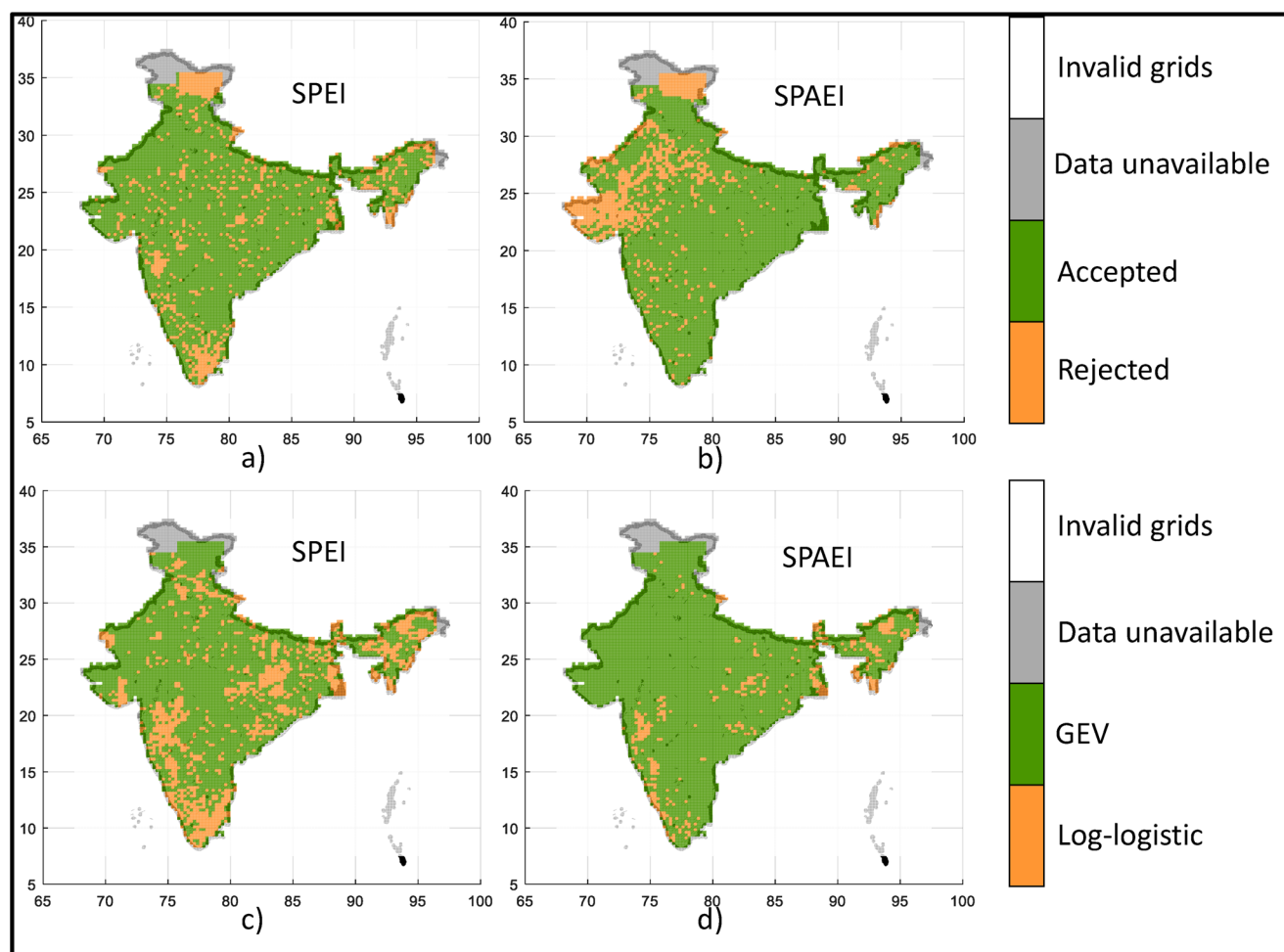


Fig. 2 a, b Results from the K–S test for all over India with accepted and rejected grid points at a significance level of 0.05 for GEV distribution for the accumulated period of 12 months for SPEI and SPAEI respectively. **c,**

d Results from AIC for best relative fit all over India for SPEI and SPAEI respectively

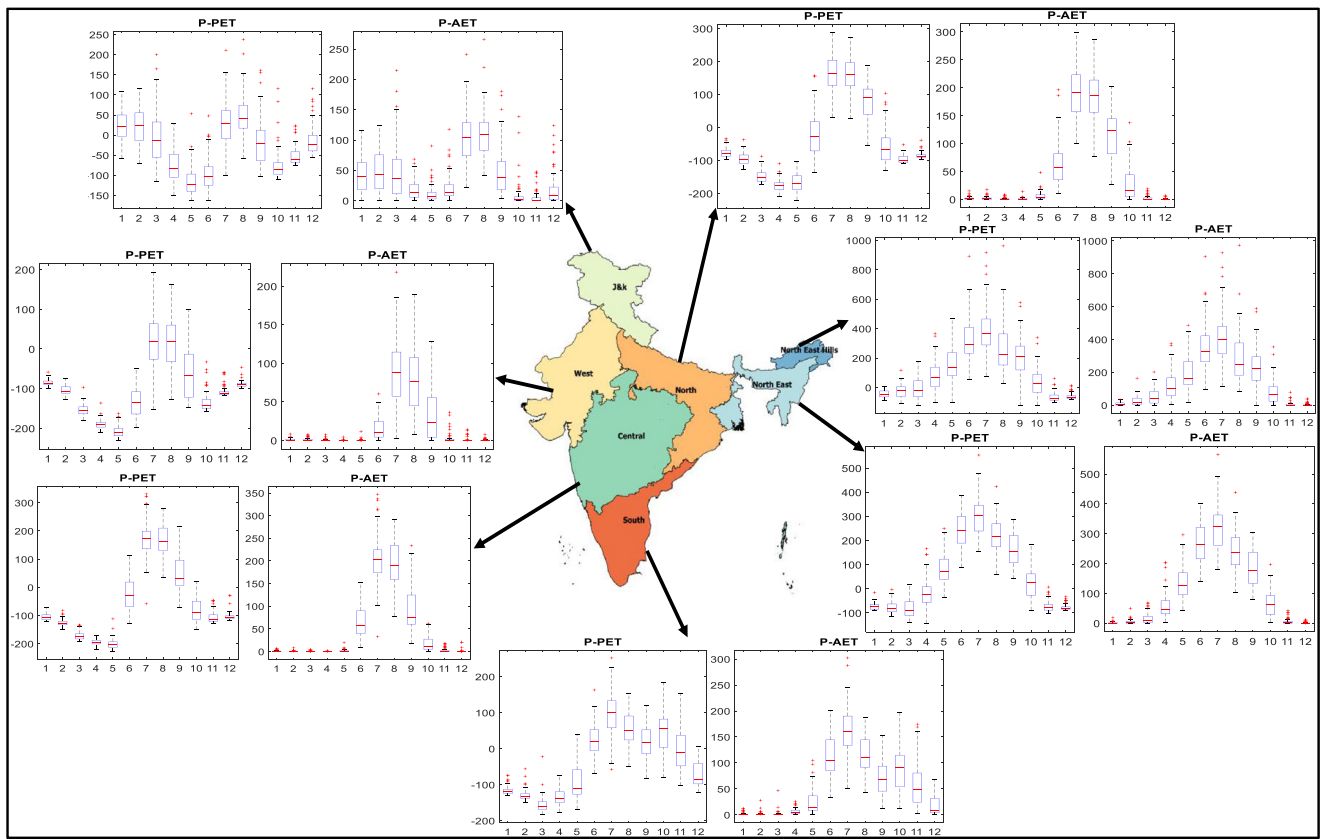


Fig. 3 Monthly spatial average of AET-based residual available water, RAW_{AET} , (P-AET), and PET-based residual available water, RAW_{PET} , (P-PET)

3 Study area and data

Fine-resolution (0.25°) daily rainfall data from the India Meteorological Department (IMD) for the period of 1901 to 2014, covering main land region of India with a spatial domain of 6.5° N to 38.5° N, and 66.5° E to 100° E (Fig. 1), was used in the study (Pai et al., 2014). Similarly, daily maximum, minimum, and mean temperature datasets at $1^\circ \times 1^\circ$ resolution for the period of 1951–2014 from IMD were used in the study (Srivastava et al., 2009). The temperature datasets were brought to a common resolution of 0.25° by bilinear interpolation. The precipitation and temperature datasets were aggregated to monthly scale to perform the analysis. A common data period of 1951 to 2014 was considered, which is further divided in to three segments (1951–1971, 1972–1992, and 1993–2013) to understand the trends and variability associated with SPEI and SPAEI drought formulations. The three time periods of 1951–1971, 1972–1992, and 1993–2013 here onwards denoted as TS1, TS2, and TS3 respectively.

Further, to proceed with the validation of the estimated AET as demonstrated in the present study, a comparison between modeled AET and remote sensing-based AET data has been carried out. For this purpose, the study adopted GLEAM satellite-based AET data which provides the land evaporation data considering the evaporation from land, soil, plant surfaces, open water and transpiration from vegetation along with dynamic land cover information and has showed high skill scores for most

of the land cover types (<https://www.gleam.eu/>) (Martens et al., 2017; Miralles et al., 2011). Due to the availability of long time series ET datasets of GLEAM for the period of 1980 to 2018 at $0.25^\circ \times 0.25^\circ$ resolution, the present study used GLEAM-based AET data to validate the estimated AET of the present study.

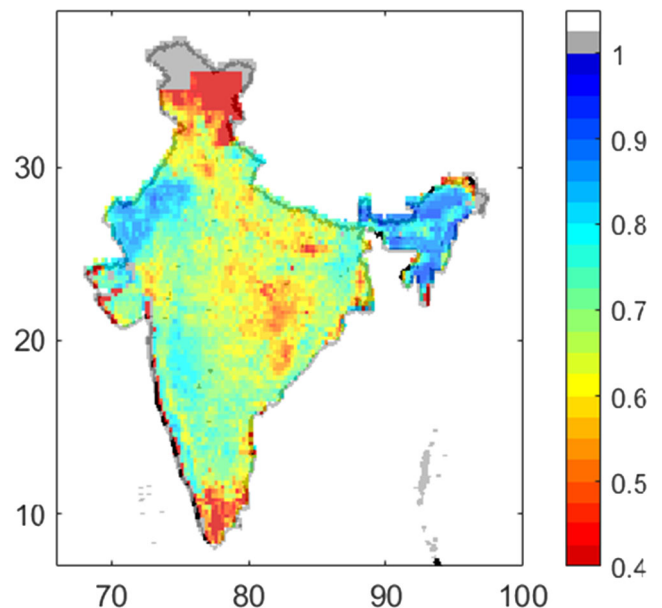


Fig. 4 Correlation coefficients between modeled (Budyko formulation) estimates of AET and remote sensing (GLEAM) data

4 Results and discussions

4.1 Construction of SPEI and SPAEI

The present study tested GEV and LL distributions for fitting the time series of RAW_{PET} and RAW_{AET} values using the K-S goodness-of-fit test. A rejection frequency based on the K-S test was defined to study the suitability of a particular distribution for fitting the time series of RAW_{PET} and RAW_{AET} for each homogeneous zone and overall India. The rejection frequency is defined as the ratio of number of grid points which did not fit the time series of RAW_{PET} or RAW_{AET} for the

selected distribution, to the total number of grid points in that region at a given significance level of 0.05. The lower the rejection frequency, the better the distribution performance in a particular region according to the K-S test. All over India, the K-S rejection frequencies were estimated as 10.0% (19.5%) and 9.1% (34.6%) with SPEI (SPA EI) respectively with GEV and LL distributions (Table 2). The GEV distribution has performed consistently better over three-parameter LL distribution to fit the time series of RAW_{PET} and RAW_{AET} according to the K-S test (Fig. 2a, b). Further, the present study used AIC relative ranking to investigate the best fitted distribution for RAW_{PET} and RAW_{AET} time series all

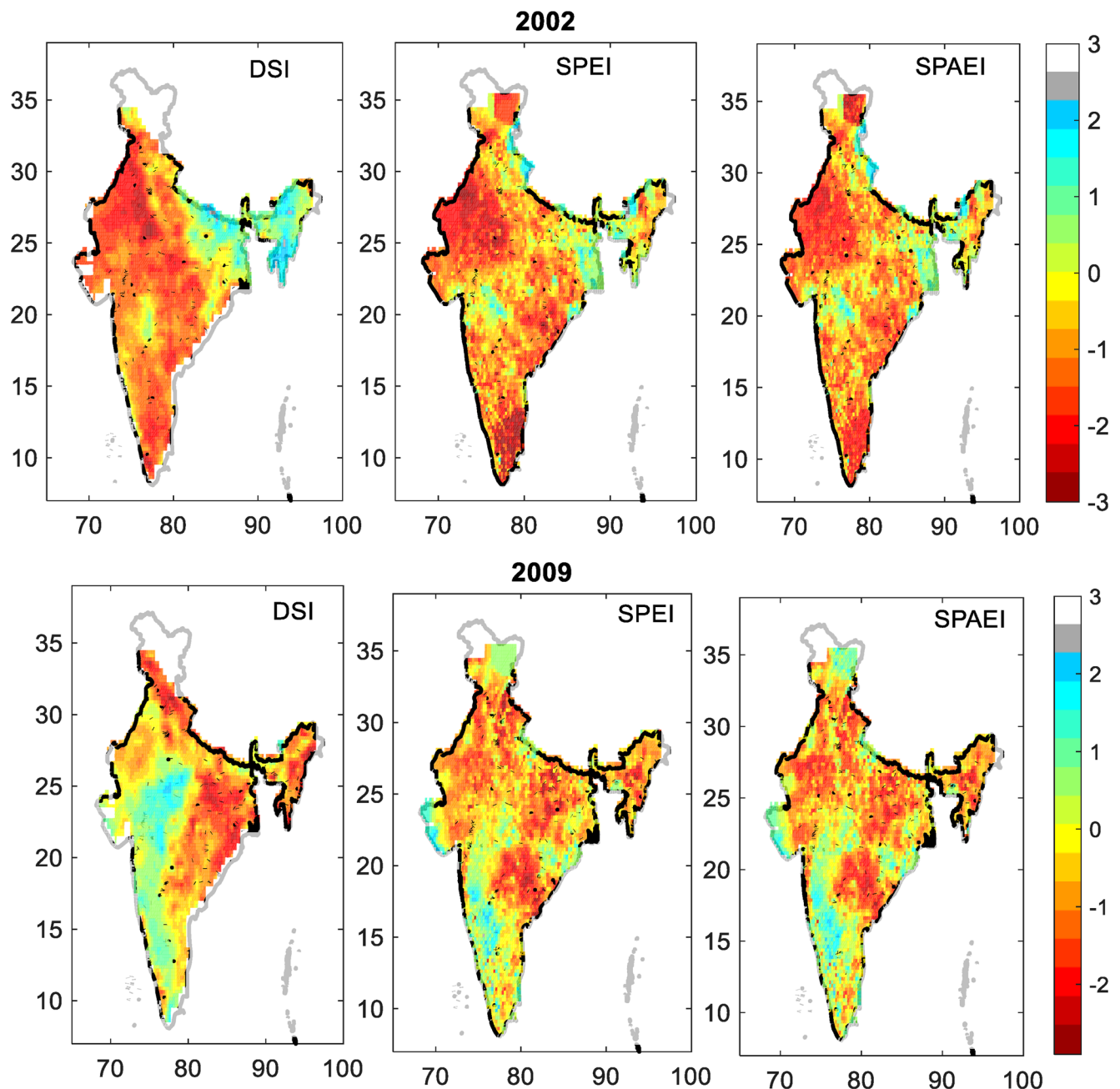


Fig. 5 Spatial comparison of SPEI and SPAEI drought intensities with DSI drought intensities for the year 2002 and 2009

over India. The AIC values were estimated for each grid point for a given probability distribution and ranked to select a best distribution based on the minimum AIC value (Fig. 2c, d). About 70 and 91% of grid points have ranked GEV distribution as the best fit for both RAW_{PET} and RAW_{AET} time series respectively at 12-month time scale. The results of the present study was consistent with the earlier research findings by Monish & Rehana (2019) on the selection of GEV distribution as the best fit for SPEI at 12-month time scale for various meteorological zones of India. Hence, the present study considered GEV distribution as the best fit for formulating SPEI and SPAEI drought study all over India.

4.2 Analysis of (P-PET) and (P-AET) for various zones of India

The study characterized each homogeneous meteorological zone as energy and water-limited zones by comparing the annual total precipitation and PET for the period of 1951 to 2014. If the annual mean $P < PET$, then the zone is defined as water-limited zone, whereas if the annual mean $P > PET$, then the region is defined as energy-limited region (Donohue et al., 2007). Based on such definition, the values of annual (P/PET) values were estimated for central (1084/1800 mm), south (1248/1695 mm), west (545/1768 mm), north (1180/1688 mm), and J&K (1025/1343 mm) and characterized as water-limited zones, whereas the northeast (2118/1473 mm) and northeast hills (2715/1434 mm) were characterized as energy-limited zones. Meanwhile, Padmakumari et al. (2013) characterized entire India as water-limited with pan evaporation and station rainfall datasets. It can be noted that the research findings of the present study were based on observed gridded precipitation and temperature datasets with modeled AET and PET estimates in the water and energy-limited zonal characterization. Such characterization will help to analyze the suitability and adoptability of PET and AET in drought analysis.

The spatial averaged monthly RAW_{PET} (P-PET) and RAW_{AET} (P-AET) for the historical data of 1951 to 2014 were compared (Fig. 3). The (P-E) is considered as a more reliable estimate and proxy to estimate the water availability (Sebastian et al., 2016). Both northeast and northeast hills zones, which are characterized as energy-limited zones, have shown similar pattern of water availabilities based on both (P-PET) and (P-AET) throughout the year. There is a considerable difference between the water availabilities of (P-PET) and (P-AET) for the water-limited zones of India (central, south, west, north, and J&K). This is evident from the assumptions adopted in the estimation of AET; as for the energy-limited zones, the AET is mainly defined by PET and for water-limited zones, the AET is mainly defined by precipitation (Sposito, 2017). Therefore, the comparison of PET and AET-based drought characterization is of more relevance for

the water-limited zones (central, south, west, north, and J&K). Though the range of values for (P-PET) and (P-AET) is different for all the zones, the pattern of values which is important for the drought index calculation is consistent for most of the zones as shown in Fig. 3. Due to the noticeable difference between (P-PET) and (P-AET), the variation of drought characterization based on SPEI and SPAEI over water-limited zones is also expected (discussed in Section 4.2).

4.3 Validation of the drought analysis with remote sensing data

Further, to proceed with the validation of the estimated AET as demonstrated in the present study, a comparison between modeled AET and remote sensing-based AET data has been performed (Fig. 4). Figure 4 shows the correlation coefficients estimated between annual AET estimated using the Budyko formulation and GLEAM-based remote sensing data for the period of 1980 to 2014. Higher correlation coefficients were observed for western and northeast zones and lower correlations for central, north, and south zones (Fig. 4). About 99% of the grid points all over India has shown correlation coefficients greater than 0.5, estimated between AET with the Budyko model and AET with remote sensing data, which shows a reasonable agreement for most part of the country. With this, the modeled AET as proposed in the present study can be valuable to predict annual droughts having the limitations towards neglected storages and fixed parametric models at monthly scale.

Further, the SPEI and SPAEI were compared with satellite-based terrestrial drought index, drought severity index (DSI) developed by Mu et al. (2012). DSI is based on the Moderate Resolution Imaging Spectroradiometer (MODIS) MOD16 ET-PET product driven by the National Centers for

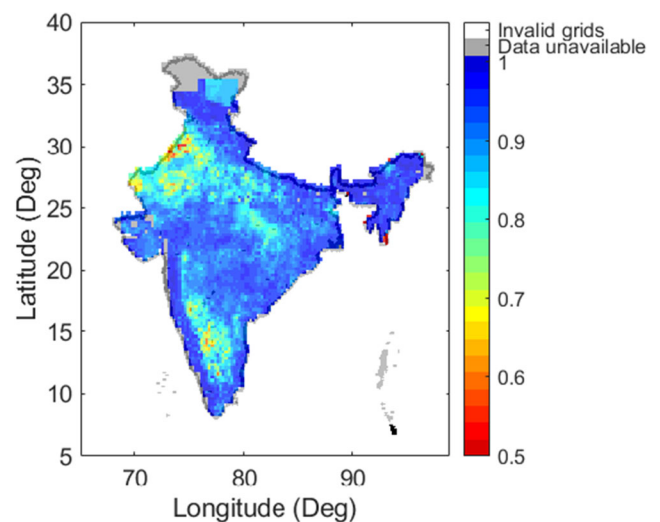


Fig. 6 Spatial correlation between SPEI and SPAEI over India for the period of 1951 to 2014 for 12-month accumulation period

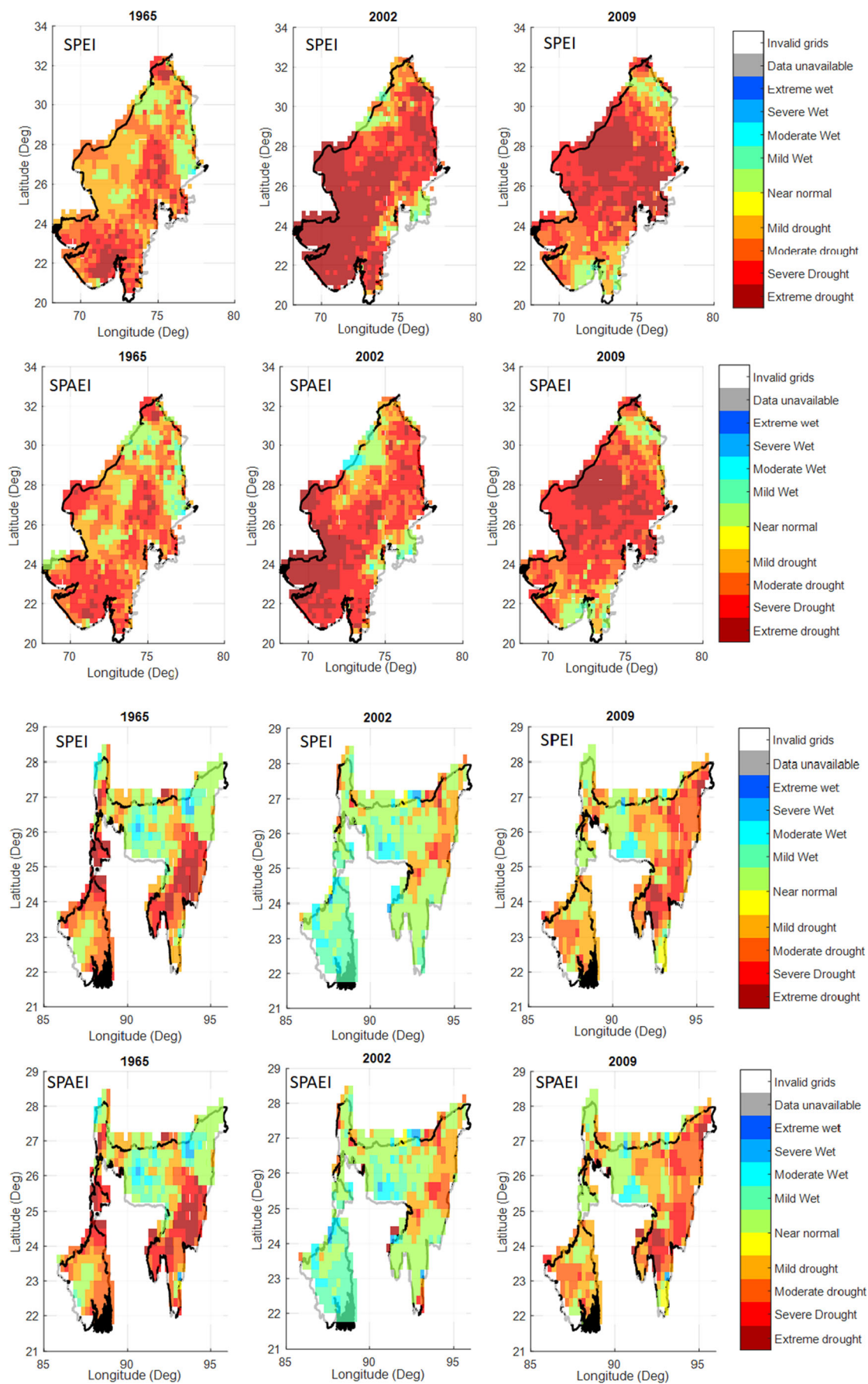


Fig. 7 Drought intensity for 1965, 2002, and 2009 drought years as estimated by SPEI (top) and SPAEI (bottom) for water-limited (western) and energy-limited (NE) regions

Environmental Prediction–Department of Energy Atmospheric Model Intercomparison Project Reanalysis II (NCEP–DOE II) (Jung et al. 2010). DSI is formulated based on normalized difference vegetation index (NDVI) data products from MODIS, which has potential to connect climate and vegetation responses (Xu et al. 2011). Furthermore, DSI has been widely applied all over the world to compare various drought indices Shah & Mishra (2020). DSI is at $0.5^\circ \times 0.5^\circ$ resolution from 2000 to 2011. The DSI data was interpolated to $0.25^\circ \times 0.25^\circ$ resolution for comparison of SPEI and SPAEI and well in agreement for the major drought years of 2002 and 2009 all over India (Fig. 5). The drought intensities of DSI is more comparable for the year 2002 compared to 2009 with both SPEI and SPAEI. Here, we have compared the intensities of DSI with SPEI and SPAEI for western and NE zones of India to show the suitability of PET and AET-based drought indices for water and energy-limited zones. The SPEI values has shown higher intensities compared to DSI and SPAEI over the western zone compared to NE. For example, the DSI intensity for a random grid ($26^\circ 75' N \times 72^\circ 75' E$) over the western zone was noted as -1.753 , the SPEI value as -2.30 , and the SPAEI value as -2.17 . Similarly, for another random grid in the western zone ($27^\circ 25' N \times 70^\circ 75' E$), the value of DSI was noted as -1.31 , the SPEI value as $-$

Table 3 Spatial averaged percentages of various drought areal extent categories for SPEI and SPAEI for all meteorologically homogeneous zones of India

Zone	Index	Drought type	1951–1971	1972–1992	1993–2013
India	SPEI	Moderate	58.87	46.77	43.07
		Severe	35.35	49.23	49.76
		Extreme	5.78	4.99	7.17
	SPAEI	Moderate	57.03	52.06	45.23
		Severe	39.54	46.14	51.49
		Extreme	3.43	1.8	3.28
NE	SPEI	Moderate	46.62	49.1	35.14
		Severe	39.86	43.92	47.75
		Extreme	13.51	6.98	17.12
	SPAEI	Moderate	49.32	50.45	37.61
		Severe	38.96	46.17	51.58
		Extreme	11.71	3.38	10.81
West	SPEI	Moderate	62.2	36.15	45.31
		Severe	36.66	61.79	51.08
		Extreme	1.13	2.06	3.60
	SPAEI	Moderate	50.26	40.89	41.71
		Severe	48.3	57.67	55.61
		Extreme	1.44	1.44	2.68

1.93, and the SPAEI value as -1.71 . It can be concluded that the SPEI values has resulted in higher drought intensities

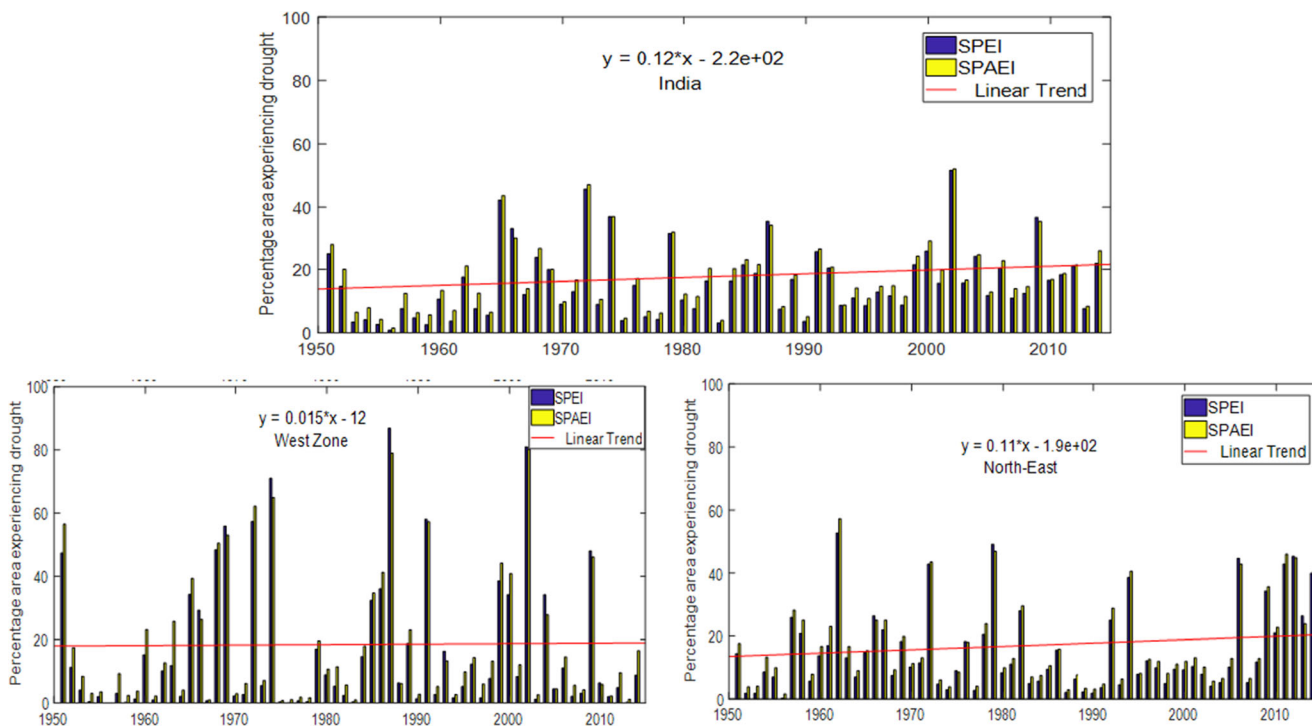


Fig. 8 Percentage of drought (SPEI/SPAEI < -1) areal extent estimated by SPEI and SPAEI for all over India, water-limited (western), and energy-limited (NE) regions along with linear trends of SPAEI for period of 1951 to 2014

compared to both DSI and SPAEI. It is also clear that SPEI being solely depends on the atmospheric evaporative demand without consideration about the actual water availabilities on the landscape, overestimating of drought intensities for the arid or water-limited regions. A similar comparison for energy-limited zone was also carried out by comparing the drought intensities for the most affected drought year of 2002 over NE region at a random grid ($28^{\circ} 00' N \times 95^{\circ} 00' E$) as -0.07 , the SPEI value as 0.32 , and the SPAEI value as 0.33 . For another random grid point ($27^{\circ} 75' N \times 94^{\circ} 25' E$) over the NE regions also, the values of DSI was found to be as 0.68 , the SPEI value as -0.48 , and the SPAEI value as -0.51 . It is clear that while the difference between DSI values compared to SPEI and SPAEI is very small, the difference between the SPEI and SPAEI values are also negligible for energy-limited regions compared to water-limited regions. Such differences are evident for water and energy-limited zones due to the model estimates of PET and AET, which is based on the assumption that for water-limited regions the AET is defined by P and for the energy-limited regions the AET is defined by PET. Therefore, the study can conclude that, for energy-limited zones, both PET and AET-based drought indices will provide the similar drought intensities, whereas for water-limited zones, the SPEI can lead to overestimates of drought intensities, for which the AET-based drought indicator is most suitable.

4.4 Comparison of spatial and temporal drought characteristics of SPEI and SPAEI

The results of the study found that SPEI and SPAEI are significantly correlated with about 97% of grid points having correlation greater than 0.95, whereas the western zone and rain shadow regions of Western Ghats in the south zone exhibited slightly lower degree of correlation with a range of 0.95 to 0.93 (Fig. 6). As the precipitation used in the drought estimation is same for both SPEI and SPAEI, the difference in the values of SPEI and SPAEI exists is only due to the variation in the values of PET and AET. Due to these differences in water availabilities (P-PET and P-AET) for water-limited zones (Fig. 3), which is evident that existence of considerable difference between the PET and AET, use of AET in the drought estimation is of relevance for the water-limited zones of India compared to energy-limited zones.

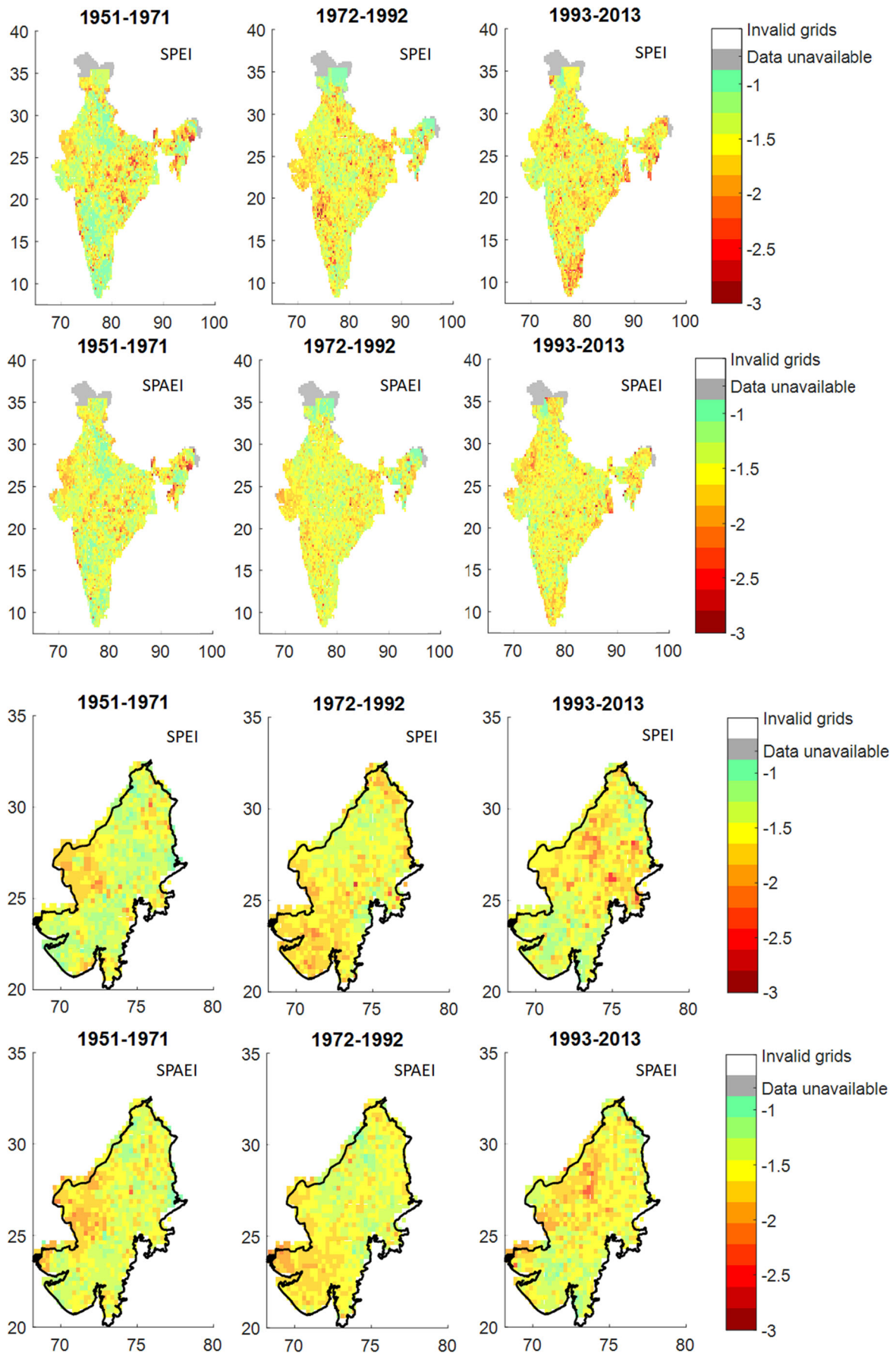
To assess SPEI and SPAEI for drought detection, the drought characteristics such as severity, frequency, duration, and areal extent of droughts for each meteorologically homogeneous zone were studied from 1951 to 2014. Also, to test the difference between PET and AET is significant enough and use of AET could provide more insights in the drought estimation, the values of SPEI and SPAEI were compared for the period of 1951 to 2014. To elaborate the significance of

PET and AET-based drought indices characterization, the study adopted one water-limited zone of western and one energy-limited zone of northeast for the comparison of drought severity, intensity, frequency, and durations.

Both SPEI and SPAEI were able to capture major droughts all over India and for each zone occurred in 1951, 1965, 1966, 1968, 1972, 1974, 1979, 1982, 1985, 1986, 1987, 2002, 2004, 2009, 2014, and 2015 (De et al. 2005; Mallya et al. 2016) (Fig. 7). To study the drought areal extents with SPEI and SPAEI, yearly drought percentage of area experiencing drought were compared for each zone. The areal extent of drought for each zone was estimated as percentage of area experiencing drought calculated based on the ratio of number of grid points with $SPEI/SPA EI < -1$ to the total number of grid points for each zone and all over India. A grid point is drought affected if $SPEI/SPA EI < -1$ to account for all categories (including moderate, severe, and extreme drought) of droughts (Fig. 8). The spatial extent of drought was observed to be increasing all over India over the period of 1951 to 2014 (Fig. 8) both with SPEI and SPAEI. Specifically, the linear trend lines for SPAEI values have shown significant positive trends with a significance level of 0.05 for central (1.7%/decade), J&K (0.26%/decade), northeast hills (3.3%/decade), northeast (1.1%/decade), north (1.9%/decade), south (1%/decade), west (0.15%/decade), and all over India (1.2%/decade) (Fig. 8). Such positive trends were also observed with SPEI for all zones.

It can be observed that the difference between drought areal extents with SPEI and SPAEI are relatively small when the drought event was defined as $SPEI/SPA EI < -1$ (Fig. 8). Therefore, the comparison of areal extents with reference to various drought categories has been done to study the effect of inclusion of PET and AET in the drought assessment of all over India and water and energy-limited zones (Table 3). For the comparison of moderate, severe, and extreme spatio-temporal drought changes, the ratio of grids in each particular category to the total number of grids in each region were compared with both drought indices of SPEI and SPAEI as given in Table 3. All over India, the severe and extreme drought percentage areal extents have been increased (Table 3), which is consistent with the earlier research findings with SPEI based on PET (Kumar et al., 2013, Mallya et al., 2016). For instance, the severe (extreme) percentage drought area of the entire country was observed to increase by 35% (6%), 48% (5%), and 50% (7%) for the periods of TS1, TS2, and TS3 respectively with SPEI, whereas for SPAEI, the severe (extreme) percentage drought area was observed as 40% (3.4%), 46% (2%), and 52% (3.3%) for the periods of TS1, TS2, and TS3 respectively. For overall India, the extreme drought affected area was noted as 5.8% (3.4%), 4.9% (1.8%), and 7.2% (3.3%) for periods of TS1,

Fig. 9 Epochal variation in average intensity of droughts with SPEI and SPAEI for all over India, water-limited (western), and energy-limited (NE) regions



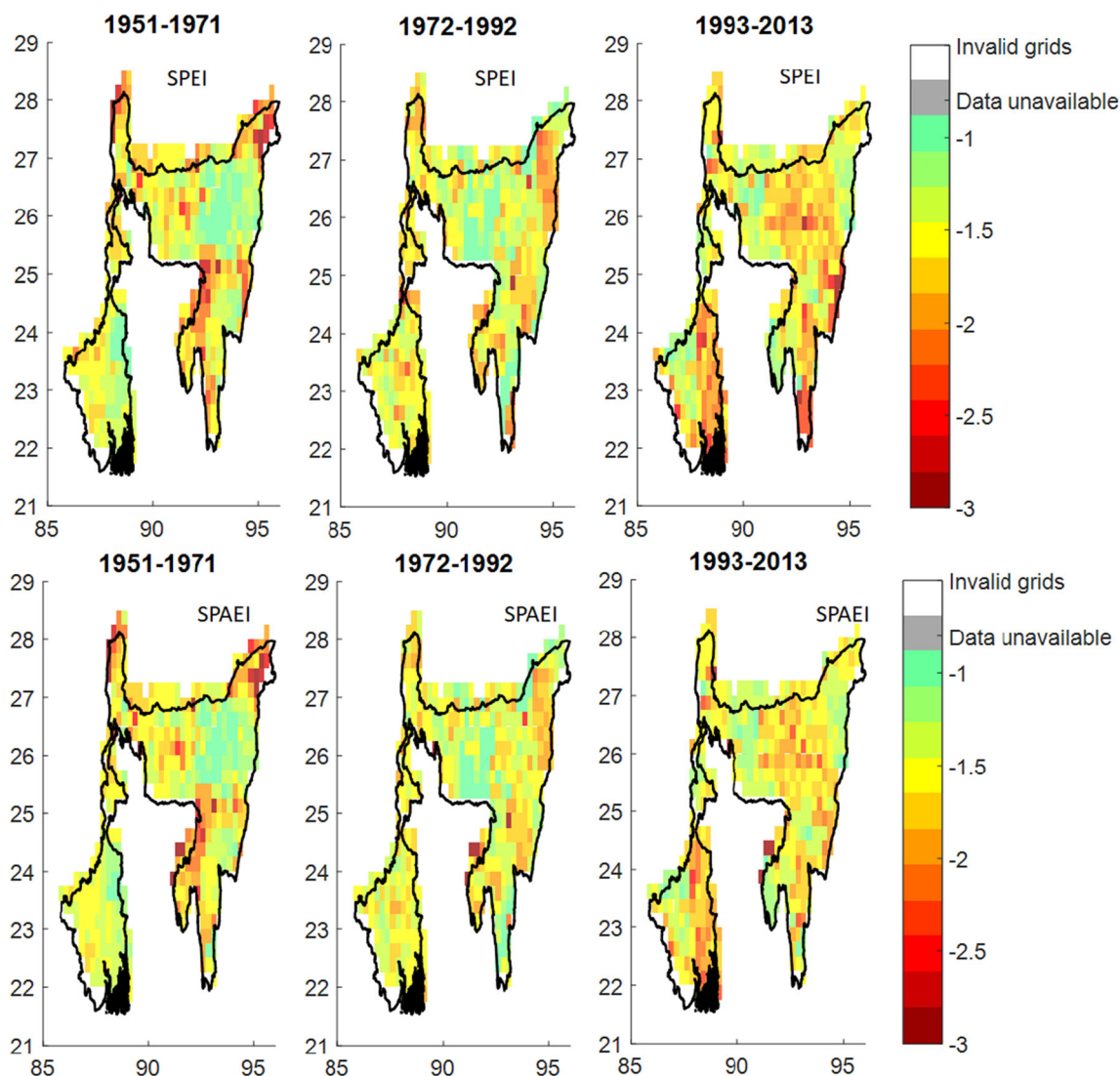


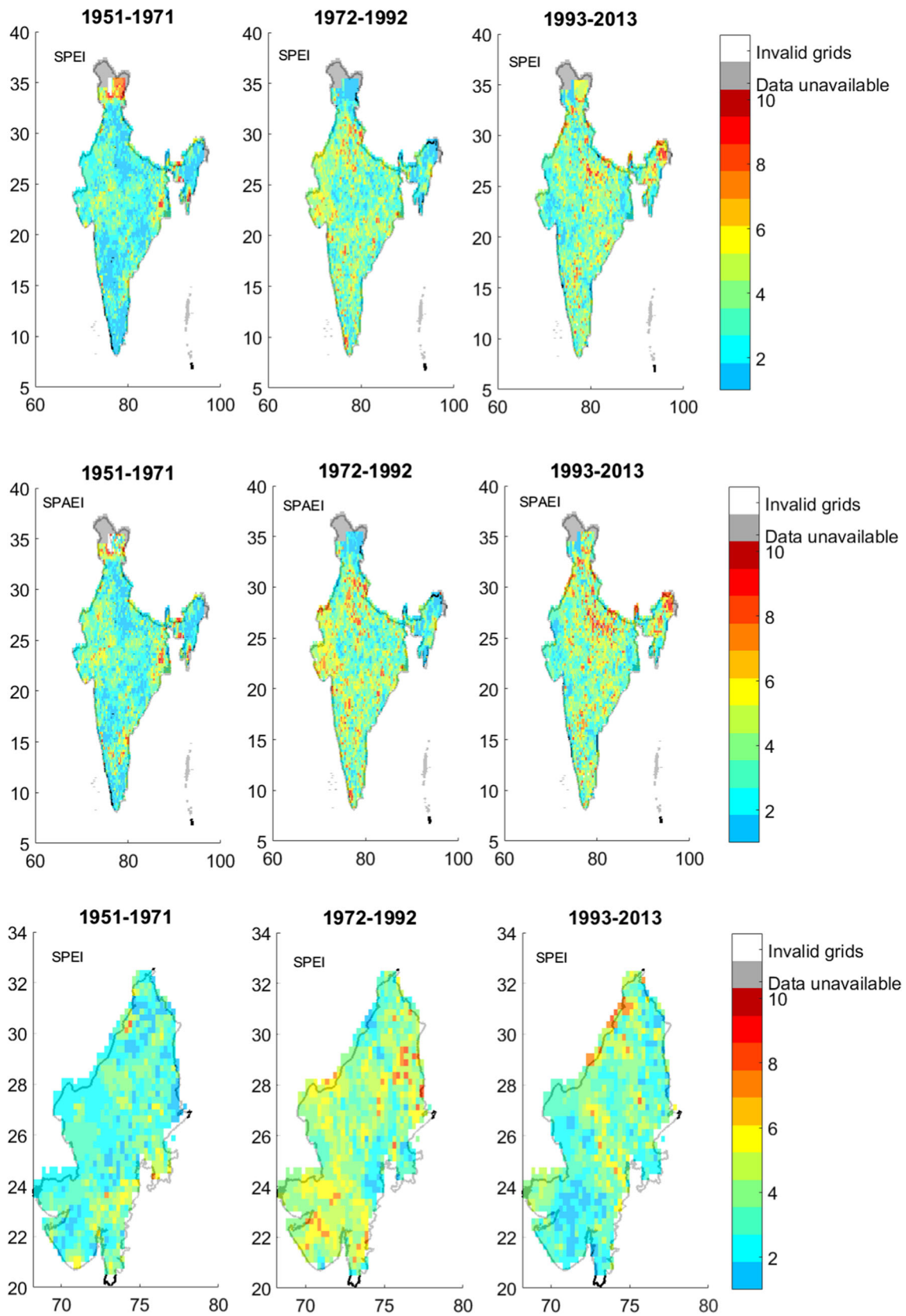
Fig. 9 (continued)

TS2, and TS3 respectively with SPEI (SPA EI). The year 2002 was identified as the most widespread drought year over India with about 52% of area affected with SPEI, in which 20.0% was moderate, 17.8% was severe, and 13.6% was extreme drought. For the same year, SPA EI has identified drought affected area as 52%, in which 20.5% was moderate, 21.5% was severe, and 11.4% was extreme drought. Here, the comparison of severity of droughts between SPEI and SPA EI reveals that the percentage of area which was categorized under extreme droughts was found to be less with SPA EI indicating lower extreme drought areal extents with SPA EI particularly for water-limited regions as shown in Fig. 7.

At zonal scale, the difference between moderate and severe drought affected areas of SPEI and SPA EI was observed to be relatively less compared to extreme droughts, for water-limited zone (Table 3). For another water-limited zone of the central zone, the area under extreme drought was noted as

6.2% (3.0%), 6.2% (1.3%), and 4.1% (1.1%) for TS1, TS2, and TS3 respectively with SPEI (SPA EI), whereas such difference between the area under extreme drought captured by SPEI and SPA EI is relatively small for energy-limited zones of the northeast (Table 3). For instance, the northeast zone, exhibited the area under extreme drought as 13.5% (11.7%), 7% (4%), and 17% (11%) for TS1, TS2, and TS3 respectively with SPEI (SPA EI). Hence, considerable difference in extreme drought affected area was noticed between SPEI and SPA EI for all water-limited zones (central, J&K, north, south, west), while such differences were not observed for energy-limited zones (northeast, northeast hills). Therefore, the

Fig. 10 Epochal variation in average frequency of droughts with SPEI and SPA EI for all over India, water-limited (western), and energy-limited (NE) regions



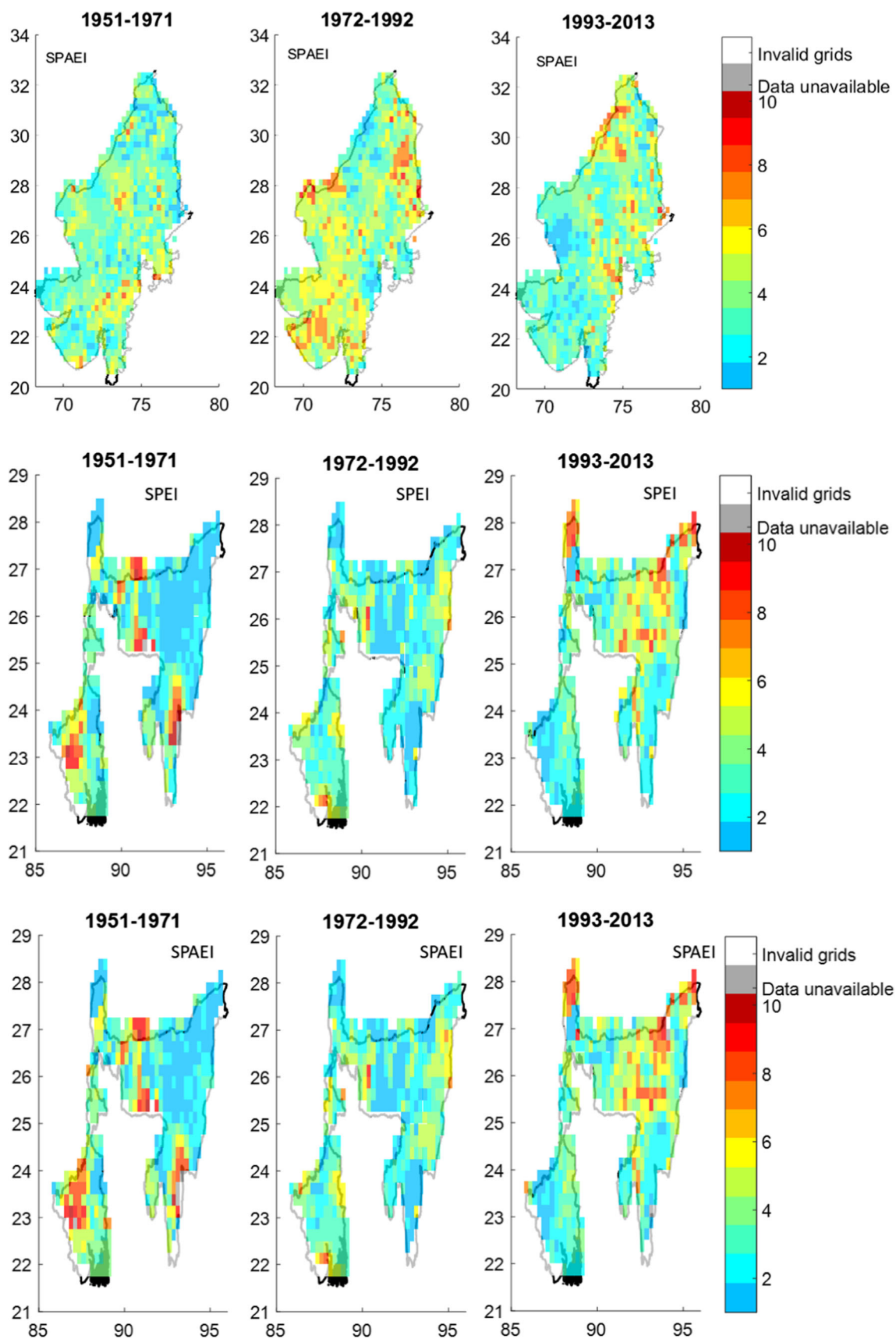


Fig. 10 (continued)

research findings of the study reveal that the use of AET in the drought categorization perhaps provide more insight towards the extreme drought event assessment for water-limited zones.

The spatio-temporal variability of SPEI and SPAEI drought indices were studied for each epoch (TS1, TS2, TS3) for all over India, western, and NE zones in terms of drought intensity (Fig. 9), frequency (Fig. 10), and duration (Fig. 11). Regarding drought intensity, for TS1, the extreme intensities of droughts were noted for north, central, and NE and only few parts of south and western zones (Fig. 8), while for TS2, more intensified droughts were observed for entire western zone, Western Ghats of the south zone, and north and NE zones of the country. Such increasing trends of drought events were also estimated by Mallya et al. (2016) for western and Deccan plateau regions with IMD data for the period of 1936 to 1970 for the 12-month time window. For the recent time epoch of TS3, intensified droughts were observed all over India with marked attention on western and south zones. More drought intensities were observed for the recent periods of 1993 to 2013 with both indices, whereas for the period of

TS3 (Fig. 9), the SPEI has estimated droughts with more intensity for NE hills, northeast, and south zones compared to SPAEI.

The spatio-temporal variation in the drought frequencies for three-time epochs for all over India, western, and NE zones are presented in Fig. 10. The frequency of droughts occurred during TS1, TS2, and TS3, for each grid, was estimated as the number of drought years under consideration with 12-month drought ending in December (SPEI/SPAEI < -1). Figure 10 showed an increase in frequency of droughts in terms of number of years over each epoch for various meteorological homogenous zones and for the country. All over India, spatial averaged frequencies were estimated for SPEI (SPAEI) as 2.6 (3.2), 3.5 (3.9), and 3.7 (4.1) years (Table 4) for TS1, TS2, and TS3 respectively. Particularly, the north zone has exhibited higher frequency of drought years for TS3 for which significant decrease in annual precipitation was observed (Chen et al., 2018). Similar trends of increase of drought events over eastern Indo-Gangetic plain of India were observed in the study of Mallya et al. (2016) for the period of 1971 to 2004

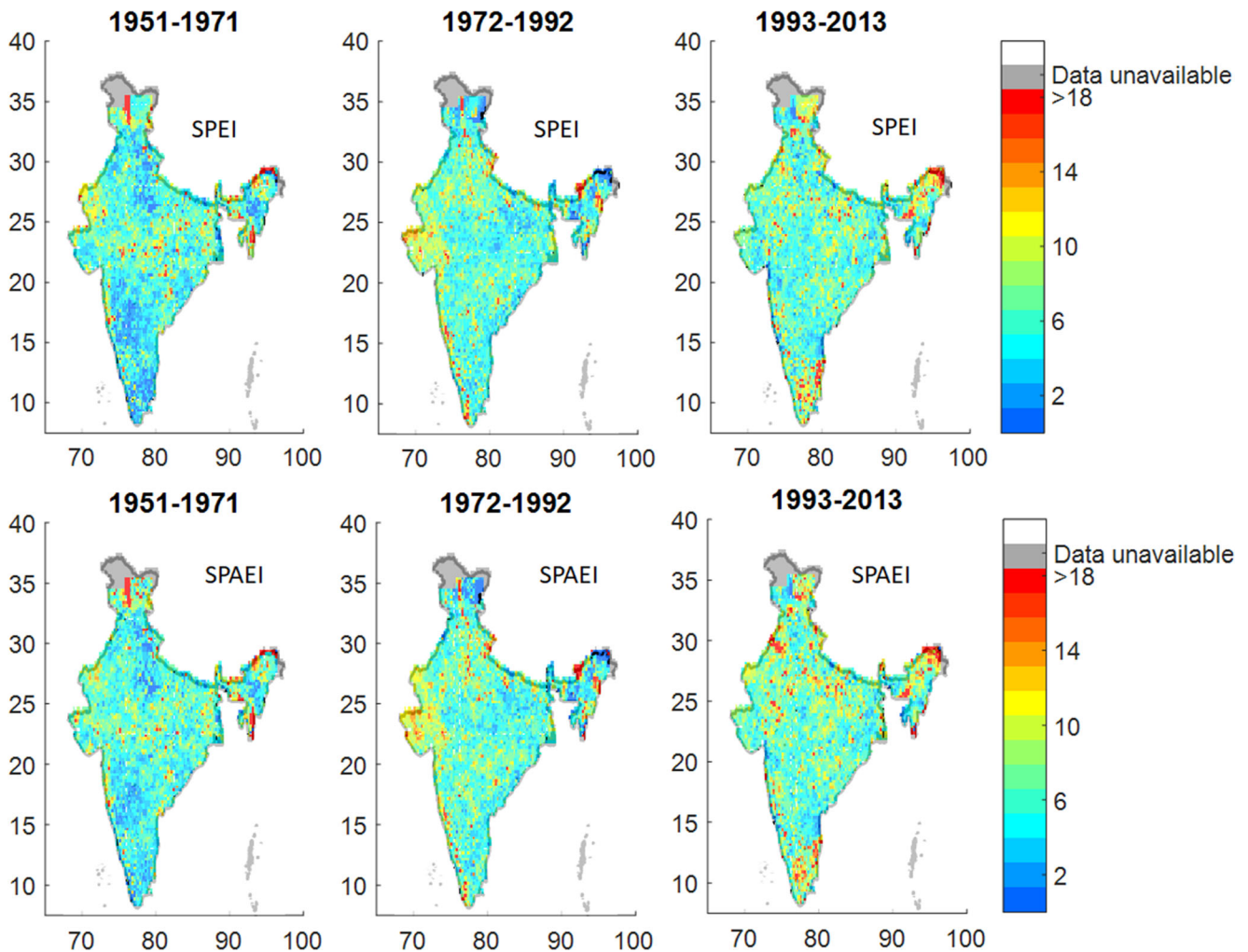


Fig. 11 Epochal variation in average duration of droughts with SPEI and SPAEI for all over India, water-limited (western), and energy-limited (NE) regions

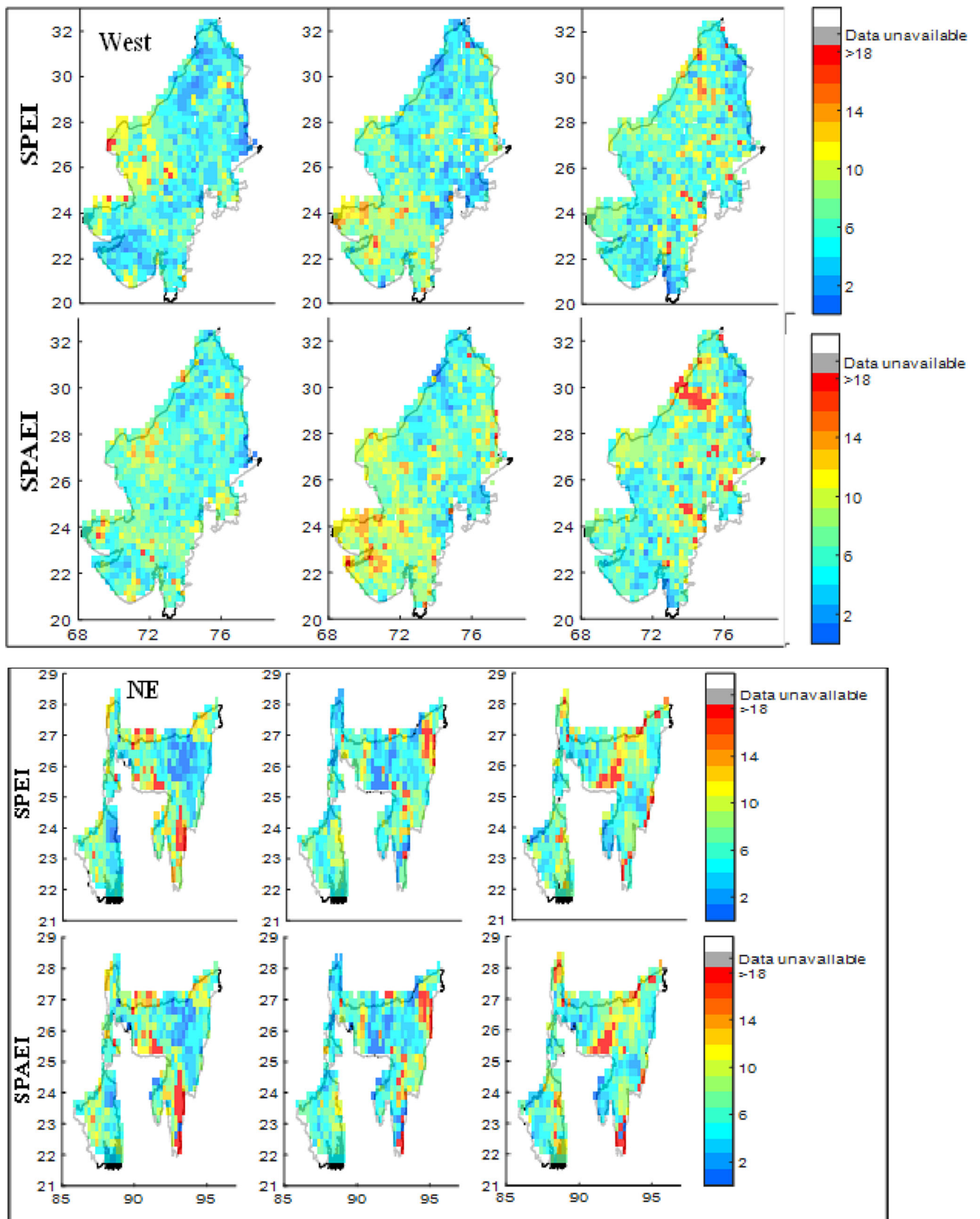


Fig. 11 (continued)

Table 4 Spatial averaged drought frequencies in years for all meteorologically homogeneous zones of India

Zone	Index	1951– 1971	1972– 1992	1993– 2013
India	SPEI	2.6	3.5	3.7
	SPA EI	3.2	3.9	4.1
NE	SPEI	3.0	2.7	3.7
	SPA EI	3.7	3.2	4.1
West	SPEI	2.8	4.3	3.2
	SPA EI	3.5	4.6	3.6

Table 6 Spatial averaged drought duration in months for all meteorologically homogeneous zones of India

Zone	Index	1951– 1971	1972– 1992	1993– 2013
India	SPEI	6.16	6.60	7.14
	SPA EI	6.62	7.06	7.75
NE	SPEI	7.24	6.49	7.72
	SPA EI	9.62	8.71	9.46
West	SPEI	6.37	7.85	6.99
	SPA EI	6.33	8.02	7.95

with SPEI. Although, the difference between the number of drought events of SPEI and SPAEI was relatively small, considerable difference between the rate of increase in the drought frequency (estimated across TS1, TS2, and TS3) has been observed. The SPEI (20.1%) has exhibited a considerable higher rate of increase in average drought frequencies compared to SPAEI (13.4%) for water-limited zone (western) compared to energy-limited zone (NE) (Fig. 10).

An analysis was made related to the drought frequencies for each category at zonal scale (Table 5). Both SPEI and SPAEI has shown an increase in the drought frequencies for all categories over India. However, the rate of increase in frequencies (estimated across TS1, TS2, and TS3) was

Table 5 Spatial averaged frequencies in months for various drought categories for SPEI and SPAEI for all meteorologically homogeneous zones of India

Zone	Index	Drought type	1951– 1971	1972– 1992	1993– 2013
India	SPEI	Moderate	19.59	23.23	24.10
		Severe	8.90	11.46	12.64
		Extreme	4.02	6.94	7.63
	SPA EI	Moderate	22.54	24.61	25.32
		Severe	12.22	16.16	17.07
		Extreme	3.89	4.87	5.83
NE	SPEI	Moderate	20.97	16.93	22.62
		Severe	9.04	8.34	11.58
		Extreme	5.48	5.28	9.16
	SPA EI	Moderate	24.94	18.37	24.94
		Severe	11.73	10.40	14.14
		Extreme	5.14	4.46	8.34
West	SPEI	Moderate	22.25	26.22	21.94
		Severe	9.54	13.97	11.27
		Extreme	3.43	9.24	5.22
	SPA EI	Moderate	24.08	24.66	20.84
		Severe	14.99	22.31	17.17
		Extreme	4.56	6.13	4.41

observed to be significantly higher in the case of extreme droughts when compared to other categories. The average rate of increase of extreme drought frequency was observed to be 40% (20%), while for severe drought as 13% (19%) and for moderate drought as 14% (4.2%) for SPEI (SPA EI) respectively for India.

The spatio-temporal variation in the drought durations for three-time epochs for each zone were presented in Fig. 11. The drought durations, in terms of number of months with SPEI/SPA EI < 1, for each drought event were estimated for the time epochs of TS1, TS2, and TS3 and for each grid point (Fig. 11). The spatial averaged drought durations were noted as 6.16 (6.62), 6.60 (7.06), and 7.14 (7.75) months (Table 6) for TS1, TS2, and TS3 respectively by SPEI (SPA EI), depicting increase of drought durations for the entire country. In particular, south, northeast, and northeast hills zones exhibited a pronounced increase in drought duration in the recent years (TS3). The research findings of the present study are in support with the study of Mallya et al. (2016), with increased drought durations over central and eastern Indo-Gangetic Plain and southern parts of India for the period of 1971–2004. The energy-limited zones (northeast and northeast hills) have exhibited considerably higher average drought durations (by ~ 20%) as estimated by SPA EI when compared to SPEI (Table 6), whereas for water-limited zones, there was negligible difference between SPEI and SPA EI in terms of drought durations. It is evident that for the water-limited zones, the AET is mainly defined by precipitation and the resultant drought indices estimated, SPA EI, is not much deviating from SPEI. Therefore, the study reveals that accurate estimation of AET, which is not only a function of precipitation and PET but also a function of vegetation, soil moisture, and open water evaporation may provide more insight towards the drought durations more accurately. However, the use of such detailed AET estimations can be a potential area of research; instead, the study aims to use more operational and readily available climate variables to formulate a drought index based on AET instead of PET which can be further used to understand the drought characterization under climate variability.

5 Advantages and limitations

The study demonstrated the restructure of a standardised PET-based drought index, SPEI, to include AET, which is modelled based on P and PET. The proposed drought indices are well in agreement with state-of-the-art of satellite-based drought indices. The study can be valuable tool for the analysis of annual droughts according to the climate and actual water availability of a region with operational meteorological data.

Despite the ability of SPAEI in capturing drought conditions over water-limited zones, it has some caveats. The major observation which was found in comparison of PET and AET-based drought estimations was differences in the drought characterization over water-limited zones compared to energy-limited zones. This is the resultant of the unique assumption which was made in the estimation of AET, when P is unlimited (energy-limited zone) AET tends to be PET and when PET is unlimited (water-limited zone) AET tends to be P . Because of this, for energy-limited regions, the dependency between SPEI and SPAEI is less compared to water-limited regions.

Secondly, SPAEI proposed in the study is based on the Budyko hypothesis (Budyko 1958) and empirical equations generated by Zhang et al. (2004), with the stationary parameter, which defines the changes in vegetation and climate change. However, a dynamic parameter of Budyko-type modelling framework can represent the joint effect of climate and land surface variability explicitly in drought assessment. In order to guarantee the relevance of AET-based drought index for Indian context and to avoid the use of short-term soil moisture storages, the focus will be only on 12-month drought. Analysis of short-term droughts are therefore beyond the scope of the present study, although they can be studied if the AET can be modelled considering monthly storage changes by adopting a hydrological model. Further, the study mainly focused on 12-month time scale (annual drought) by neglecting the storage changes and seasonality of root zone. Employing a land surface hydrological model to simulate AET accounting for storage changes and to include the dynamic parameter Budyko-type structure can be potential future research problem. Secondly, the evaporative demand estimation of SPAEI is accounted for variability of temperatures alone. Given the declining rates of global wind speed, the evaporative demand gradually decreases. Hence, the PET model used can be improved by adopting the Penman–Monteith PET model which can include various meteorological variables, such as wind speed, relative humidity, and radiation. However, due to the unavailability of such operational gridded meteorological datasets for Indian case study, the present study is limited to use the Hargreaves model for the estimation of evaporative demand for the Indian drought analysis. Further studies could improve the drought assessment framework presented here with better AET and PET estimates, which are most difficult variables to measure and deserve more attention towards the measurement in the regional water balance assessment.

To overcome such major limitation of the proposed drought indices, most accurate estimates of AET should be used in the formulation of SPAEI. One such possibility is to use the most dependable satellite-based remote sensing AET estimates. However, use of remote sensing-based AET estimates provides limitations over the validation and spatio-temporal resolutions. Also, remote sensing-based data based on AET estimates can be useful for understanding the drought variability for historical periods but limited to implement for the future scenarios. Therefore, the proposed drought formulation can be still valuable to study the projected drought characteristics under climate change due to its dependency over the most dependable projections of precipitation and temperatures from any climate model.

6 Conclusions

The study stressed on the relevance of use of AET instead of PET in the drought analysis for water-limited zones compared to energy-limited zones of India. A drought-monitoring framework was developed based on the Budyko hypothesis which allowed the study to estimate AET with readily available climate data. The drought index developed is dependent on the water available for the actual evaporative demand with reference to AET and precipitation using the structure of a SPEI. The AET-based drought index was consistent with conventional PET-based drought index in identifying the historical droughts for the meteorological homogeneous zones of India. The study compared the drought assessment with PET and AET for various meteorological homogeneous zones of India, which are characterised as water and energy-limited zones. The central, south, west, north, and J&K are identified as water-limited zones and NE and NE hills as energy-limited zones. Furthermore, the present study noted GEV distribution as the most promising in formulating the SPEI and SPAEI for India in contrary with the original formulation of SPEI with log–logistic distribution. Considerable difference in extreme drought affected area was noticed between SPEI and SPAEI for all water-limited zones, while such differences were not observed for energy-limited zones. Further, higher percentage of area was categorized under extreme/severe conditions with SPEI, which was identified as severe/moderate respectively as compared with SPAEI for all water-limited zones. The energy-limited zones have exhibited considerably higher average drought durations (by $\sim 20\%$) as estimated by SPAEI when compared to SPEI. The study observed that inclusion of AET in the drought characterization instead of PET has not affected the drought frequencies but the rate of increase of drought frequency was higher in case of SPAEI. Overall, the study reveal that the use of AET in the drought categorization perhaps provides more insight towards the drought intensity assessment for water-limited zones of India.

Acknowledgments The authors acknowledge India Meteorological Department, Pune, for providing gridded data of precipitation and temperatures.

Funding The research work is partially supported by Science and Engineering Research Board (SERB), Department of Science and Technology, Government of India, through Start-up Grant for Young Scientists (YSS) Project No. YSS/2015/002111 to Dr. S. Rehana.

References

- Aadhar, S. & Mishra, V. (2017) High-resolution near real-time drought monitoring in South Asia. *Sci Data* **4**(1), 1–14. Nature Publishing Group. doi:<https://doi.org/10.1038/sdata.2017.145>
- Akaike, H. (1974) A new look at the statistical model identification. *IEEE Trans Autom Control* **19**(6), 716–723. Presented at the IEEE Transactions on Automatic Control. doi:<https://doi.org/10.1109/TAC.1974.1100705>, A new look at the statistical model identification
- Anabalón A, Sharma A (2017) On the divergence of potential and actual evapotranspiration trends: an assessment across alternate global datasets. *Earth's Future* **5**(9):905–917. <https://doi.org/10.1002/2016EF000499>
- Bai, P., Liu, X., Zhang, D. & Liu, C. (2020) Estimation of the Budyko model parameter for small basins in China. *Hydrol Process* **34**(1), 125–138. John Wiley & Sons, Ltd. doi:<https://doi.org/10.1002/hyp.13577>
- Beguéría S, Vicente-Serrano SM, Reig F, Latorre B (2014) Standardized precipitation evapotranspiration index (SPEI) revisited: parameter fitting, evapotranspiration models, tools, datasets and drought monitoring. *Int J Climatol* **34**(10):3001–3023. <https://doi.org/10.1002/joc.3887>
- Brutsaert, W. (1982) *Evaporation into the atmosphere: theory, history and applications*. Springer Netherlands doi:<https://doi.org/10.1007/978-94-017-1497-6>
- Budyko M (1974) *Climate and life*. Academic Press, New York
- Buytaert W, Bièvre BD (2012) Water for cities: the impact of climate change and demographic growth in the tropical Andes. *Water Resour Res* **48**(8). <https://doi.org/10.1029/2011WR011755>
- Chen, W.-T., Huang, K.-T., Lo, M.-H. & LinHo, L. H. (2018) Post-monsoon season precipitation reduction over South Asia: impacts of anthropogenic aerosols and irrigation. *Atmosphere* **9**(8), 311. Multidisciplinary Digital Publishing Institute. doi:<https://doi.org/10.3390/atmos9080311>, Post-Monsoon Season Precipitation Reduction over South Asia: Impacts of Anthropogenic Aerosols and Irrigation
- Choudhury BJ (1999) Evaluation of an empirical equation for annual evaporation using field observations and results from a biophysical model. *J Hydrol* **216**(1):99–110. [https://doi.org/10.1016/S0022-1694\(98\)00293-5](https://doi.org/10.1016/S0022-1694(98)00293-5)
- Dai, A. (2011) Drought under global warming: a review. *Wiley Interdisciplinary Reviews Climate Change* Wiley doi:<https://doi.org/10.1002/wcc.81>, 2, 45, 65
- Donohue RJ, Roderick ML, McVicar TR (2007) On the importance of including vegetation dynamics in Budyko's hydrological model. *Hydrol Earth Syst Sci* **13**
- El Kenawy, A., Vicente-Serrano, S. M., Angulo, M., Lopez-Moreno, J. I. & Beguería, S. (2010) A new global 0.5° gridded dataset (1901–2006) of a multiscalar drought index: comparison with current drought index datasets based on the palmer drought severity index. *J Hydrometeorol. American Meteorological Society*. doi:10.1175/2010JHM1224.1
- Hargreaves GH (1975) Moisture availability and crop production. *Trans ASAE* **18**(5):0980–0984. <https://doi.org/10.13031/2013.36722>
- Hargreaves GH, Allen RG (2003) History and evaluation of Hargreaves evapotranspiration equation. *J Irrig Drain Eng* **129**(1):53–63. [https://doi.org/10.1061/\(ASCE\)0733-9437\(2003\)129:1\(53\)](https://doi.org/10.1061/(ASCE)0733-9437(2003)129:1(53))
- Homdee T, Pongput K, Kanae S (2016) A comparative performance analysis of three standardized climatic drought indices in the Chi River basin, Thailand. *Agric Nat Resour* **50**(3):211–219. <https://doi.org/10.1016/j.anres.2016.02.002>
- Jensen ME, Burman RD, Allen RG (1990) Evapotranspiration and irrigation water requirements 360–360. ASCE Retrieved from <https://cedb.asce.org/CEDBsearch/record.jsp?dockkey=0067841>
- Joetzer, E., Douville, H., Delire, C., Ciaia, P., Decharme, B. & Tyteca, S. (2013) Hydrologic benchmarking of meteorological drought indices at interannual to climate change timescales: a case study over the Amazon and Mississippi river basins. *Hydrol Earth Syst Sci* **17**(12), 4885–4895. Copernicus GmbH. doi: <https://doi.org/10.5194/hess-17-4885-2013>
- Jung, M., Reichstein, M., Ciaia, P., Seneviratne, S. I., Sheffield, J., Goulden, M. L., Bonan, G., et al. (2010) Recent decline in the global land evapotranspiration trend due to limited moisture supply. *Nature* **467**(7318), 951–954. Nature Publishing Group. doi:<https://doi.org/10.1038/nature09396>
- Kalma JD, McVicar TR, McCabe MF (2008) Estimating land surface evaporation: a review of methods using remotely sensed surface temperature data. *Surv Geophys* **29**(4):421–469. <https://doi.org/10.1007/s10712-008-9037-z>
- Kim D, Rhee J (2016) A drought index based on actual evapotranspiration from the Bouchet hypothesis. *Geophys Res Lett* **43**(19):10, 277–10,285. <https://doi.org/10.1002/2016GL070302>
- Kumar, K. N., Rajeevan, M., Pai, D. S., Srivastava, A. K. & Preethi, B. (2013) On the observed variability of monsoon droughts over India. *Weather and Climate Extremes* **1**. Elsevier BV. Retrieved from <https://cyberleninka.org/article/n/1038610>
- Liu M, Xu X, Xu C, Sun AY, Wang K, Scanlon BR, Zhang L (2017) A new drought index that considers the joint effects of climate and land surface change. *Water Resour Res* **53**(4):3262–3278. <https://doi.org/10.1002/2016WR020178>
- Liu S, Yan D, Wang H, Li C, Weng B, Qin T (2016) Standardized Water Budget Index and Validation in Drought Estimation of Haihe River Basin, North China. In: Standardized Water Budget Index and validation in drought estimation of Haihe River basin, North China. *Advances in Meteorology*. Research article, Hindawi. <https://doi.org/10.1155/2016/9159532>
- Mallya G, Mishra V, Niyogi D, Tripathi S, Govindaraju RS (2016) Trends and variability of droughts over the Indian monsoon region. *Weather Clim Extremes* **12**:43–68. <https://doi.org/10.1016/j.wace.2016.01.002>
- Martens, B., Miralles, D. G., Lievens, H., Schalie, R. van der, Jeu, R. A. M. de, Fernández-Prieto, D., Beck, H. E., Dorigo W. A., Verhoest N. E. C. (2017) GLEAM v3: satellite-based land evaporation and root-zone soil moisture. *Geosci Model Dev* **10**(5), 1903–1925. Copernicus GmbH. doi: <https://doi.org/10.5194/gmd-10-1903-2017>
- McKee TB, Doesken NJ, Kleist J (1993) The relationship of drought frequency and duration to time scales. In Proceedings of the. In: 8th Conference on Applied Climatology. Boston, MA: American Meteorol Soci **17** (22), pp 179–183
- Miralles, D. G., Holmes, T. R. H., Jeu, R. A. M. D., Gash, J. H., Meesters, A. G. C. A. & Dolman, A. J. (2011) Global land-surface evaporation estimated from satellite-based observations. *Hydrol Earth Syst Sci* **15**(2), 453–469. Copernicus GmbH. doi: <https://doi.org/10.5194/hess-15-453-2011>
- Monish NT, Rehana S (2019) Suitability of distributions for standard precipitation and evapotranspiration index over meteorologically homogeneous zones of India. *J Earth Syst Sci* **129**(1):25. <https://doi.org/10.1007/s12040-019-1271-x>

- Mu, Q., Zhao, M., Kimball, J. S., McDowell, N. G. & Running, S. W. (2012) A Remotely Sensed Global Terrestrial Drought Severity Index. *Bull Amer Meteor Soc* **94**(1), 83–98. American Meteorological Society. doi:<https://doi.org/10.1175/BAMS-D-11-00213.1>
- Mueller B, Seneviratne SI, Jimenez C, Corti T, Hirschi M, Balsamo G, Ciaia P, Dirmeyer P, Fisher JB, Guo Z, Jung M, Maignan F, McCabe MF, Reichle R, Reichstein M, Rodell M, Sheffield J, Teuling AJ, Wang K, Wood EF, Zhang Y (2011) Evaluation of global observations-based evapotranspiration datasets and IPCC AR4 simulations. *Geophys Res Lett* **38**(6). <https://doi.org/10.1029/2010GL046230>
- Nath R, Cui X, Nath D, Graf HF, Chen W, Wang L, Gong H, Li Q (2017) CMIP5 multimodel projections of extreme weather events in the humid subtropical Gangetic Plain region of India. *Earth's Future* **5**(2):224–239. <https://doi.org/10.1002/2016EF000482>
- Padmakumari, B., Jaswal, A. K. & Goswami, B. N. (2013) Decrease in evaporation over the Indian monsoon region: implication on regional hydrological cycle. *Clim Chang* **121**(4), 787–799. Springer. Retrieved from <http://link.springer.com/article/10.1007%2Fs10584-013-0957-3>
- Pai, D. S., Sridhar, L., Rajeevan, M. C., Sreejith, O. P., Satbhai, N. S. & Mukhopadhyay, B. (2014) Development of a new high spatial resolution ($0.25^\circ \times 0.25^\circ$) long period (1901–2010) daily gridded rainfall data set over India and its comparison with existing data sets over the region.
- Schrier, G. van der, Jones, P. D. & Briffa, K. R. (2011) The sensitivity of the PDSI to the Thornthwaite and Penman-Monteith parameterizations for potential evapotranspiration. *J Geophys Res-Atmos* **116**(D3). doi:<https://doi.org/10.1029/2010JD015001>
- Sebastian, D. E., Pathak, A. & Ghosh, S. (2016) Use of atmospheric budget to reduce uncertainty in estimated water availability over South Asia from different reanalyses. *Sci Rep* **6**(1), 1–10. Nature Publishing Group. doi:<https://doi.org/10.1038/srep29664>
- Shah D, Mishra V (2020) Integrated Drought Index (IDI) for drought monitoring and assessment in India. *Water Resour Res* **56**(2): e2019WR026284. <https://doi.org/10.1029/2019WR026284>
- Sheffield J, Wood EF, Roderick ML (2012) Little change in global drought over the past 60 years. *Nature* **491**(7424):435–438. <https://doi.org/10.1038/nature11575>
- Shelton, M. L. (2008) *Hydroclimatology: perspectives and applications*. Cambridge Core Cambridge University Press doi:<https://doi.org/10.1017/CBO9780511754746>
- Sienz, F., Bothe, O. & Fraedrich, K. (2012) Monitoring and quantifying future climate projections of dryness and wetness extremes: SPI bias. *Hydrol Earth Syst Sci* **16**(7), 2143–2157. Copernicus GmbH. doi: <https://doi.org/10.5194/hess-16-2143-2012>
- Spinoni J, Barbosa P, De Jager A, McCormick N, Naumann G, Vogt JV, Magni D et al (2019) A new global database of meteorological drought events from 1951 to 2016. *J Hydrol* **22**:100593. <https://doi.org/10.1016/j.jhr.2019.100593>
- Sposito, G. (2017) Understanding the Budyko equation. *Water* **9**(4), 236. Multidisciplinary Digital Publishing Institute. doi:<https://doi.org/10.3390/w9040236>
- Srivastava AK, Rajeevan M, Kshirsagar SR (2009) Development of a high resolution daily gridded temperature data set (1969–2005) for the Indian region. *Atmos Sci Lett* **10**(4):249–254. <https://doi.org/10.1002/asl.232>
- Stagge JH, Tallaksen LM, Gudmundsson L, Loon AFV, Stahl K (2015) Candidate distributions for climatological drought indices (SPI and SPEI). *Int J Climatol* **35**(13):4027–4040. <https://doi.org/10.1002/joc.4267>
- Stagge, J. H., Tallaksen, L. M., Xu, C. Y. & Lanen, H. A. J. V. (2014) Standardized precipitation-evapotranspiration index (SPEI): sensitivity to potential evapotranspiration model and parameters, Vol. 363, 367–373. Presented at the Hydrology in a Changing World. Retrieved from <https://library.wur.nl/WebQuery/wurpubs/558281>
- Svoboda, M., LeCompte, D., Hayes, M., Heim, R., Gleason, K., Angel, J., Rippey, B., et al. (2002) The drought monitor. & ULL. AM. METEOROL. SOC. **83**(8), 1181–1190. American Meteorological Society. doi: [https://doi.org/10.1175/1520-0477\(2002\)083<1181:TDM>2.3.CO;2](https://doi.org/10.1175/1520-0477(2002)083<1181:TDM>2.3.CO;2)
- Vicente Serrano SM, Beguería S, López-Moreno JI (2010) A multi-scalar drought index sensitive to global warming: the standardized precipitation evapotranspiration index – SPEI. *Am Meteorol Soc*. <https://doi.org/10.1175/2009JCLI2909.1>
- Wang H, Chen Y, Pan Y, Chen Z, Ren Z (2019) Assessment of candidate distributions for SPI/SPEI and sensitivity of drought to climatic variables in China. *Int J Climatol* **39**(11):4392–4412. <https://doi.org/10.1002/joc.6081>
- Xu L, Samanta A, Costa MH, Ganguly S, Nemani RR, Myneni RB (2011) Widespread decline in greenness of Amazonian vegetation due to the 2010 drought. *Geophys Res Lett* **38**(7). <https://doi.org/10.1029/2011GL046824>
- Zhang L, Hickel K, Dawes WR, Chiew FHS, Western AW, Briggs PR (2004) A rational function approach for estimating mean annual evapotranspiration. *Water Resour Res* **40**(2). <https://doi.org/10.1029/2003WR002710>
- Zhou S, Yu B, Huang Y, Wang G (2015) The complementary relationship and generation of the Budyko functions. *Geophys Res Lett* **42**(6):1781–1790. <https://doi.org/10.1002/2015GL063511>

Publisher's note Springer Nature remains neutral with regard to jurisdictional claims in published maps and institutional affiliations.